Acta Neuropathologica (2019) 137:879–899
https://doi.org/10.1007/s00401-019-01962-9

ORIGINAL PAPER

Genome-wide analyses as part of the international FTLD-TDP whole-genome sequencing consortium reveals novel disease risk factors and increases support for immune dysfunction in FTLD

Cyril Pottier[1] · Yingxue Ren[2] · Ralph B. Perkerson III[1] · Matt Baker[1] · Gregory D. Jenkins[3] · Marka van Blitterswijk[1] · Mariely DeJesus-Hernandez[1] · Jeroen G. J. van Rooij[4] · Melissa E. Murray[1] · Elizabeth Christopher[1] · Shannon K. McDonnell[3] · Zachary Fogarty[3] · Anthony Batzler[3] · Shulan Tian[3] · Cristina T. Vicente[1] · Billie Matchett[1] · Anna M. Karydas[5] · Ging-Yuek Robin Hsiung[6] · Harro Seelaar[4] · Merel O. Mol[4] · Elizabeth C. Finger[7] · Caroline Graff[8,9] · Linn Öijerstedt[8,9] · Manuela Neumann[10,11] · Peter Heutink[10,12] · Matthis Synofzik[10,12] · Carlo Wilke[10,12] · Johannes Prudlo[10,13] · Patrizia Rizzu[10] · Javier Simon-Sanchez[10,12] · Dieter Edbauer[14,15] · Sigrun Roeber[16] · Janine Diehl-Schmid[17] · Bret M. Evers[18] · Andrew King[19,20] · M. Marsel Mesulam[21] · Sandra Weintraub[21,22] · Changiz Geula[21] · Kevin F. Bieniek[1,23] · Leonard Petrucelli[1] · Geoffrey L. Ahern[24] · Eric M. Reiman[25] · Bryan K. Woodruff[26] · Richard J. Caselli[26] · Edward D. Huey[27] · Martin R. Farlow[28] · Jordan Grafman[29] · Simon Mead[30] · Lea T. Grinberg[5,31] · Salvatore Spina[5] · Murray Grossman[32] · David J. Irwin[32] · Edward B. Lee[33] · EunRan Suh[33] · Julie Snowden[34] · David Mann[35] · Nilufer Ertekin-Taner[1,36] · Ryan J. Uitti[36] · Zbigniew K. Wszolek[36] · Keith A. Josephs[37] · Joseph E. Parisi[37] · David S. Knopman[37] · Ronald C. Petersen[37] · John R. Hodges[38] · Olivier Piguet[39] · Ethan G. Geier[5] · Jennifer S. Yokoyama[5] · Robert A. Rissman[40,41] · Ekaterina Rogaeva[42] · Julia Keith[43,44] · Lorne Zinman[43] · Maria Carmela Tartaglia[42,45] · Nigel J. Cairns[46] · Carlos Cruchaga[47] · Bernardino Ghetti[48] · Julia Kofler[49] · Oscar L. Lopez[50,24] · Thomas G. Beach[51] · Thomas Arzberger[52,14,16] · Jochen Herms[14,16] · Lawrence S. Honig[53] · Jean Paul Vonsattel[54] · Glenda M. Halliday[38,55] · John B. Kwok[38,55] · Charles L. White III[18] · Marla Gearing[56] · Jonathan Glass[56] · Sara Rollinson[57] · Stuart Pickering-Brown[57] · Jonathan D. Rohrer[58] · John Q. Trojanowski[33] · Vivianna Van Deerlin[33] · Eileen H. Bigio[21] · Claire Troakes[19] · Safa Al-Sarraj[19,20] · Yan Asmann[2] · Bruce L. Miller[5] · Neill R. Graff-Radford[36] · Bradley F. Boeve[37] · William W. Seeley[5,31] · Ian R. A. Mackenzie[59] · John C. van Swieten[4] · Dennis W. Dickson[1] · Joanna M. Biernacka[3] · Rosa Rademakers[1]

Received: 3 December 2018 / Revised: 11 January 2019 / Accepted: 12 January 2019 / Published online: 9 February 2019

Abstract

Frontotemporal lobar degeneration with neuronal inclusions of the TAR DNA-binding protein 43 (FTLD-TDP) represents the most common pathological subtype of FTLD. We established the international FTLD-TDP whole-genome sequencing consortium to thoroughly characterize the known genetic causes of FTLD-TDP and identify novel genetic risk factors. Through the study of 1131 unrelated Caucasian patients, we estimated that *C9orf72* repeat expansions and *GRN* loss-of-function mutations account for 25.5% and 13.9% of FTLD-TDP patients, respectively. Mutations in *TBK1* (1.5%) and other known FTLD genes (1.4%) were rare, and the disease in 57.7% of FTLD-TDP patients was unexplained by the known FTLD genes. To unravel the contribution of common genetic factors to the FTLD-TDP etiology in these patients, we conducted a two-stage association study comprising the analysis of whole-genome sequencing data from 517 FTLD-TDP patients and

Electronic supplementary material The online version of this article (https://doi.org/10.1007/s00401-019-01962-9) contains supplementary material, which is available to authorized users.

Extended author information available on the last page of the article

838 controls, followed by targeted genotyping of the most associated genomic loci in 119 additional FTLD-TDP patients and 1653 controls. We identified three genome-wide significant FTLD-TDP risk loci: one new locus at chromosome 7q36 within the *DPP6* gene led by rs118113626 (p value = 4.82e − 08, OR = 2.12), and two known loci: *UNC13A*, led by rs1297319 (p value = 1.27e − 08, OR = 1.50) and *HLA-DQA2* led by rs17219281 (p value = 3.22e − 08, OR = 1.98). While *HLA* represents a locus previously implicated in clinical FTLD and related neurodegenerative disorders, the association signal in our study is independent from previously reported associations. Through inspection of our whole-genome sequence data for genes with an excess of rare loss-of-function variants in FTLD-TDP patients ($n \geq 3$) as compared to controls ($n = 0$), we further discovered a possible role for genes functioning within the *TBK1*-related immune pathway (e.g., *DHX58*, *TRIM21*, *IRF7*) in the genetic etiology of FTLD-TDP. Together, our study based on the largest cohort of unrelated FTLD-TDP patients assembled to date provides a comprehensive view of the genetic landscape of FTLD-TDP, nominates novel FTLD-TDP risk loci, and strongly implicates the immune pathway in FTLD-TDP pathogenesis.

Keywords Whole-genome sequencing FTLD-TDP · TBK1 · DPP6 · UNC13A · HLA · Immunity

Introduction

Frontotemporal lobar degeneration (FTLD) is one of the leading causes of dementia in individuals younger than 65 years but can also affect individuals later in life. In the past two decades, a number of monogenic causes and genetic risk factors of FTLD have been described. Mutations in the genes encoding microtubule-associated protein tau (*MAPT)* and progranulin (*GRN*), and repeat expansions in the chromosome 9 open reading frame 72 (*C9orf72)* gene were identified as the most common genetic causes of FTLD [4, 17, 38]; however, the majority of patients remain genetically unexplained. FTLD is an umbrella term for a highly heterogeneous group of clinical syndromes that result from selective dysfunction and typically atrophy of the frontal and temporal lobes. The predominant clinical presentations of FTLD are behavior and language dysfunction resulting in behavioral variant (bvFTD) [75], semantic variant of primary progressive aphasia (svPPA) or agrammatic variant of primary progressive aphasia (agPPA) [32]; however, related clinical syndromes such as frontotemporal dementia with motor neuron disease (FTD-MND), progressive supranuclear palsy (PSP) syndrome, and corticobasal syndrome (CBS) can occur. Patients with FTLD may further present with psychiatric symptoms and conditions such as compulsive behavior, mood disorders, and schizophrenia [102]. FTLD neuropathological studies have also revealed heterogeneity and pathological classification is now defined by the main component of the protein aggregates in a patient's brain at post mortem examination. FTLD with neuronal and cytoplasmic aggregates of the DNA and RNA-binding protein TDP-43 (FTLD-TDP) is most common and based on the distribution of the neuronal cytoplasmic TDP-43-positive inclusions and dystrophic neurites in the cortical layers, at least five distinct FTLD-TDP pathological subtypes (A–E) are described [45, 55]. Interestingly, while the nature of the underlying FTLD pathology is challenging to predict in most clinically diagnosed FTLD patients, mutations in *GRN* invariably lead to FTLD-TDP type A, while repeat expansions in *C9orf72* are mainly associated with FTLD-TDP type B [54]. In contrast, patients with mutations in *MAPT* accumulate pathological tau proteins (FTLD-tau) and do not have FTLD-TDP pathology [9]. These correlations between specific gene mutations and pathology subgroups provides validation for the pathological classification system and suggests that, at least in part, distinct molecular pathways could contribute to disease in the various FTLD pathological subtypes. Consequently, genetic studies focused on large clinical cohorts may have reduced power due to undesirable heterogeneity and analysis of specific FTLD pathological subtypes may be beneficial. Indeed, the inclusion of clinical patients in genome-wide association study (GWAS) has been successful by identifying one genome-wide significant association signal for FTLD at the HLA locus on chromosome 6 but required more than 2000 FTLD patients and 4000 controls [27]. On the contrary, the use of a much smaller cohort of pathologically confirmed FTLD-TDP patients identified *TMEM106B* as a genetic risk factor [86]. The latter study, however, was performed more than 8 years ago, only focused on common genetic variants, and included a significant number of patients with pathogenic *GRN* mutations and repeat expansions in *C9orf72*, underscoring the need for additional studies.

Here, we present the results of our newly established International FTLD-TDP whole-genome sequencing (WGS) consortium, in which we identified more than 1150 unrelated pathologically confirmed FTLD-TDP patients from 23 participating sites. Genome-wide association studies in 517 Caucasian FTLD-TDP patients without mutations in the known genes and 838 controls identified common risk variants at one novel (*DPP6*) and two known loci (*UNC13A* and *HLA-DQA2*) and suggest that rare damaging variants in the *TBK1*-related innate immune pathway are enriched in FTLD-TDP patients as compared to controls. These findings extend the genetic landscape of FTLD-TDP and further highlight immune dysfunction as a potential contributing factor in the development of FTLD-TDP.

Methods

Study subjects and basic genetic and pathological characterization

International FTLD-TDP whole-genome sequencing (WGS) Consortium

To identify novel genetic factors implicated in FTLD-TDP, we established the International FTLD-TDP WGS Consortium. Previously ascertained FTLD-TDP patients from 23 European, North American and Australian participating sites were included, one patient per family (Table 1). The pathological diagnosis of FTLD-TDP was considered sufficient for inclusion, irrespective of the clinical diagnosis of the patient. Patients diagnosed with FTLD-TDP and concomitant signs of motor neuron disease were also included. The availability of DNA for basic genetic characterization was considered an additional inclusion criterion such that the presence of a *C9orf72* expansion could be determined in all patients, mutations in *GRN* could be determined in all FTLD-TDP type-A patients and *VCP* could be screened in all FTLD-TDP type-D patients. For those patients in which mutation status was not yet available at the start of the study, *C9orf72* repeat expansions were analyzed using our previously reported two-step protocol and Sanger sequencing was used for *GRN* and *VCP* mutation screening [4, 21, 97]. Information on the presence of known disease mutations in other neurodegenerative disease genes within the cohort was requested from all participating sites but not all patients were systematically screened. A total of 1134 Caucasian and 20 non-Caucasian FTLD-TDP patients were identified.

Discovery cohort

The discovery stage included 554 genetically unexplained self-declared Caucasian FTLD-TDP patients with sufficient DNA quality and quantity available for WGS. Participating sites were required to provide the FTLD-TDP pathological subtyping for each patient according to the harmonized classification system or had to provide unstained fixed tissue slides such that phospho-TDP-43 immunostaining could be performed as part of this study. WGS was also available for 982 control individuals from the Mayo Clinic Biobank which is a convenience population collected at Mayo Clinic with detailed clinical records on each participant (Table 2) [68]. After quality control measures (see below), 517 FTLD-TDP patients and 838 controls were included in the genetic analyses.

Replication cohort

For the replication stage, a total of 119 FTLD-TDP patients were available, including both newly ascertained FTLD-TDP patients and patient samples who failed quality control measures at the discovery stage, e.g. low coverage and low call rate (Table 2). FTLD-TDP patient samples from the discovery stage who failed quality control measures due to contamination, race, sex error or duplicates were not selected for the replication cohort. FTLD-TDP patients known to be related to individuals included in the discovery cohort were excluded. Similar to the discovery cohort, all patients were negative for *C9orf72* repeat expansions and FTLD-TDP type-A patients were negative for mutations in *GRN*. A total of 1653 controls including a set of 249 pathologically confirmed normal controls as well as 1404 clinical controls free of neurodegenerative disorder were used as the control cohort. Patients and controls were all reported Caucasian and originated from multiple sites (Table 2, suppl. table 2 Online Resource 1).

WGS discovery cohort

Whole blood- or brain-derived DNA from 499 of the 554 unrelated FTLD-TDP patients from the discovery cohort and 982 individuals from the Mayo Clinic Biobank Study were whole-genome sequenced at HudsonAlpha. Approximately, 1000 ng DNA from each sample was sheared on a Covaris LE220 focused-ultrasonicator (Woburn, MA, USA) with a target yield of 350 bp fragment size. Following sonication, the fragmented DNA was taken into standard library preparation protocol using NEBNext® DNA Library Prep Master Mix Set for Illumina® (New England BioLabs Inc., Ipswich, MA, USA) with slight modifications. The post-ligated samples were individually barcoded with unique in-house primers and amplified through 6 cycles of PCR using KAPA HiFi HotStart Ready Mix (Kapa Biosystems, Inc., Woburn, MA, USA). Concentration of the libraries was assessed by Qubit® 2.0 Fluorometer, and the quality of the libraries was estimated by a DNA 5 K chip on a Caliper GX. Accurate quantification was determined using the qPCR-based KAPA Biosystems Library Quantification kit (Kapa Biosystems, Inc., Woburn, MA, USA). Each sample was sequenced on one lane of Illumina's HiSeq X instrument using v2 flow cells and reagents to target 30× genomic coverage. Fastq files previously generated on an Illumina HiSeq X for 55 FTLD-TDP patients were obtained from 3 sites: UCSF ($n=36$) [31], DZNE ($n=14$) and NSW ($n=5$) leading to a total of 554 FTLD patients whole-genome sequenced.

For all FTLD-TDP patients and controls, fastq files were transferred to Mayo Clinic and processed through the Mayo Genome GPS v4.0 pipeline in batches of up to 75 samples.

Table 1 Overview of genetic status in FTLD-TDP patients within the international FTLD-TDP whole-genome sequencing consortium

Site	Number of FTLD-TDP	Caucasian					Non-Caucasian				
		Non mutation carriers	*GRN*	*C9orf72*	*TBK1*	Other genes	Non mutation carriers	*GRN*	*C9orf72*	*TBK1*	Other genes
Banner Sun Health Research Institute	29	20	6	3	0	0	0	0	0	0	0
Columbia University	25	20	2	3	0	0	0	0	0	0	0
Emory University	48	26	6	13	0	0	1	1	1	0	0
Erasmus University	93	63	5	22	0	2	1	0	0	0	0
German Center for Neurodegenerative Diseases	24	14	2	7	1	0	0	0	0	0	0
Indiana University	32	14	13	4	1	0	0	0	0	0	0
Karolinska University	44	18	4	20	1	1	0	0	0	0	0
King's College London	50	40	3	6	0	0	1	0	0	0	0
Ludwig-Maximilians-University Munich	40	16	4	16	1	3	0	0	0	0	0
Mayo Clinic Jacksonville/Rochester	207	128	27	51	1	0	0	0	0	0	0
Northwestern University	69	44	16	8	1	0	0	0	0	0	0
University College London	54	28	13	13	0	0	0	0	0	0	0
University of British Columbia	72	31	9	26	0	0	5	1	0	0	0
University of California San Diego	15	10	2	3	0	0	0	0	0	0	0
University of New South Wales	47	16	9	20	0	2	0	0	0	0	0
University of Pennsylvania	95	41	17	29	3	2	3	0	0	0	0
University of San Francisco	101	65	9	22	1	0	1	2	1	0	0
University of Toronto	18	11	1	5	0	1	0	0	0	0	0
University of Pittsburgh Medical Center	20	15	2	3	0	0	0	0	0	0	0
University Texas Southwestern Medical Center	41	27	5	9	0	0	0	0	0	0	0
Washington University School of Medicine	24	17	2	4	0	0	1	0	0	0	0
University of Western Ontario	6	3	0	2	0	0	1	0	0	0	0
Total	1154	667 (58.8%)	157 (13.8%)	289 (25.5%)	10 (0.9%)	11 (1.0%)	14 (70.0%)	4 (20.0%)	2 (10.0%)	0	0

The genetic status of FTLD-TDP patients per site per ethnicity is presented for each of the major FTLD-TDP genes (*GRN*, *C9orf72*, *TBK1*) and for other genes which includes *VCP* ($n=5$), *CHMP2B* ($n=1$), *CHCHD10* ($n=2$), *FUS* ($n=1$), CSF1R ($n=1$) and *TIA1* ($n=1$)

Table 2 Demographics of FTLD-TDP patients and controls included in the association studies. Median age at onset, age at death and age at last healthy visit of patients and controls included in the discovery and replication stages are presented

Group	Discovery				Replication			
	Age at onset* (IQR)	Age at death (IQR)	% Female (N)	Total	Age at onset* (IQR)	Age at death (IQR)	% Female (N)	Total
FTLD-TDP	63 (56.0–70.0)	71 (64.0–78.0)	68.7% (226)	554	59 (52.0–66.0)	71 (64.0–75.6)	42.0% (50)	119
Controls	66 (57.1–76.3)	NA	50.0% (491)	982	68.1 (58.7–80.5)	NA	48.4% (800)	1653

N number of individuals, *IQR* interquartile range, *NA* not applicable, *: indicates the age at last visit for the controls

Briefly, reads were mapped to the human reference sequence (GRCh38 build) using the Burrows–Wheeler Aligner, and local realignment around indels was performed using the Genome Analysis Toolkit (GATK) [47, 57]. Variant calling was performed using GATK HaplotypeCaller followed by variant recalibration (VQSR) according to the GATK best practice recommendations [23, 87].

WGS data quality assessment

Sample level quality control

Samples with less than 30× coverage in more than 50% of the genome ($n = 17$ patients, $n = 41$ controls), call rate below 85% ($n = 1$ patient, $n = 0$ controls), sex error ($n = 4$ patients, $n = 2$ controls) or contamination defined by a FREEMIX score above 0.03 ($n = 6$ patients, $n = 4$ controls) were removed. Non-Caucasian samples ($n = 6$ patients, $n = 3$ controls) were also removed. At this step, joint genotyping on all samples was performed, a final relatedness measurement was calculated using PREST [58], and duplicate samples ($n = 3$ patients, $n = 0$ control) as well as related ones ($n = 0$ patient, $n = 25$ controls) were removed. In total, 517 pathologically confirmed FTLD-TDP samples and 907 controls passed all quality control measures. After removing 69 controls with a possible clinical diagnosis or family history of a neurodegenerative disorder as per clinical chart review, 517 FTLD-TDP patients and 838 controls were included in genetic association analyses.

Variant level quality control

Genotype calls with GQ < 10 and/or depth (DP) < 10 were set to missing, and variants with ED > 4 were removed from all subsequent analyses. For all analyses, only variants that pass VQSR and with a call rate > 95% were considered unless otherwise specified. The transition/transversion ratio for this final variant call set is 2.04. Functional annotation of variants was performed using ANNOVAR (version2016Feb01) [95]. Genotypes generated at the discovery phase for the top single nucleotide polymorphisms (SNPs, rs118113626, rs17219281 and rs12973192) were validated by independent Taqman assays (C_11514504_10 for rs12973192—custom assays were designed for rs118113626 and rs17219281) on 466 FTLD-TDP patients and 837 controls included in the discovery phase with DNA available. All genotypes from the whole-genome sequencing phase were confirmed by an orthogonal method. In addition, rs4726389 and rs118113626 were Sanger sequenced in a subset of 46 FTLD-TDP patients and 46 controls from the discovery phase and all genotypes were confirmed (primers available upon request). Rare loss of function variants (frameshift insertion/deletion/block substitution, stopgain, stoploss and splicing single nucleotide variants—SNVs) in *TBK1*, *TRIM21*, *DHX58*, *IRF7*, *IRF8*, *IRF3* and *NOD2* were confirmed by Sanger sequencing (primers available upon request).

Genotyping replication cohort

13 suggestive loci ($p < 1e-05$) were nominated for follow-up in the replication stage. For all suggestive loci, the lead variant and/or one proxy were/was included in a multiplex MassArray design (Agena Bioscience, San Diego, CA, USA) leading to a maximum of two variants per loci at the design stage. Two loci failed the design (rs148048968, rs3952538). Twenty nanograms of DNA as measured by spectrophotometer (Nanodrop; Wilmington, DE, USA) was used for genotyping on the MassArray iPLEX system (Agena Bioscience, San Diego, CA, USA) following the manufacturer's protocol. Variants with a call rate < 95% or failing Hardy–Weinberg equilibrium in controls ($p < 0.05$) were subsequently removed from the analysis (one variant, rs9818987). Both genome-wide significant *DPP6* variants and one variant at each other locus (either the lead variant or a proxy) were retained for statistical analysis resulting in a total of 11 loci. Individuals with a genotyping rate < 95% were removed from the analysis.

RNAseq analysis

RNA from frontal cortex tissue of 44 FTLD-TDP patients without known gene mutations and 24 pathologically confirmed normal controls was extracted using the RNeasy Plus mini kit (Qiagen, Venlo, Netherlands). RNA quality and quantity were determined with an Agilent 2100 Bioanalyzer using the RNA Nano Chip (Agilent Technologies). Only high-quality RNA samples were included (median RNA integrity number (RIN) = 9.3, IQR = 8.8–9.8). Library preparation was performed using Illumina TruSeq mRNA v2 prep and sequenced at 10 samples/lane as paired-end 101 base pair reads on the HiSeq 4000 (Illumina, San Diego, CA). Raw RNAseq reads were aligned to the human reference genome (GRCh38) using the spliced transcripts alignment to a reference (STAR, v2.5.2b) [26]. Library quality was assessed using the RSeQC (v3.0.0) package [96]. Gene-level expression was quantified using the feature Counts command in the Subread package (v1.5.1) [50]. An in-house R pipeline was used to obtain differentially expressed genes. Briefly, the R pipeline includes conditional quantile normalization (CQN), principal component (PC) analysis, source of variation (SOV) analysis, and differential expression analysis of genes. Differential expression analysis was performed using multivariable linear regression models adjusted for potential confounders. A Benjamini–Hochberg FDR correction was used for multiple testing. Analyses were performed with or without the incorporation of surrogate markers for five major cell types as covariates: neurons (*ENO2*), microglia (*CD68*), astrocytes (*GFAP*), oligodendrocytes (*OLIG2*), and endothelial cells (*CD34*), as described elsewhere [3, 19, 33]. All analyses also included the following covariates: RIN, sex, age, and plate.

DPP6 mRNA expression analyses

mRNA expression analysis of *DPP6* was conducted in one FTLD-TDP patient carrying a possible LOF variant and two neuropathologically normal controls in which *DPP6* LOF variants were excluded. RNA was extracted and quality was measured as described before. All RNA obtained had a RIN > 8 and was subsequently reverse transcribed using the Superscript III system (Life Technologies, Carlsbad, CA, USA). Quantitative real-time PCR was performed in quadruplicate for each sample on an ABI7900 PCR system (Applied Biosystems, Foster City, CA, USA), using TaqMan gene expression assays (Life Technologies, Carlsbad, CA, USA) and following the manufacturer's recommendations. *DPP6* transcripts were measured using the probe Hs00736294_m1 for all *DPP6* transcripts from Invitrogen (Carlsbad, CA, USA). *MAP2* (probe Hs00258900_m1) and *GAPDH* (probe Hs02758991_g1) were used as reference genes. Results were analyzed using SDS software version 2.2 (Life Technologies, Carlsbad, CA, USA). *DPP6* transcript levels were assessed using the ΔΔCt method normalized by the geometric mean of *MAP2* and *GAPDH* transcripts to account for both total cell number and the contribution of neuronal cells specifically. In addition, after reverse transcription, a cDNA fragment containing the splice site mutation as well as two known common variants (rs2293353 and rs2230064) was amplified by PCR and Sanger sequenced from the patient carrying the potential LOF *DPP6* variant and one healthy control. The presence of heterozygous status for rs2293353 and rs2230064 was confirmed at the gDNA level by Sanger sequencing (primers are available upon request).

Statistical analyses

Age at onset, death and survival after onset analyses

Distribution of ages at onset, ages at death and survival after onset were compared across pathological FTLD-TDP subgroups in the discovery phase using a Kruskal–Wallis test followed by a post hoc Dunn's test. *p* values of the Dunn's test are provided after Bonferroni correction.

Generation of principal components

Prior to running genetic association analyses, PC analysis was performed using a subset of variants meeting the following criteria: minor allele frequency (MAF) > 5% and full sample Hardy–Weinberg Equilibrium (HWE) $p > 1e-5$. For the PC analysis and common variant genome-wide association analyses, multi-allelic variants were split into multiple variables (i.e., rows in the genotype dataset), where each variable/row represents the count of a specific alternate allele with samples carrying other alternate alleles being set to missing. Influential regions such as the HLA region were removed, and SNPs were pruned by LD with r^2 threshold of 0.1 prior to PC analysis. This analysis identified 4 PCs that were significantly associated with patient control status, which were subsequently used as covariates in all genetic association analyses.

SNP-level analysis of common variants

For the common variant GWAS, SNPs with MAF > 0.01 in patients or controls and HWE $p > 1e-6$ in controls were analyzed. Multi-allelic markers were encoded as described above. In addition, since WGS of FTLD-TDP patients was performed at HudsonAlpha in 5 batches, a test was performed to identify SNPs with significant differences in genotype distributions between sequencing batches, and SNPs showing evidence of batch effects ($p < 0.05$) were removed.

For all remaining variants, association of genotypes with the patient/control status was assessed using logistic regression with allele dosage as the predictor assuming log-additive allele effects. Sex and the first four PCs were included as covariates in the models. Following the primary analysis comparing SNP genotypes between all FTLD-TDP patients and controls, exploratory analyses within pathological FTLD-TDP strata were performed to evaluate SNP association with FTLD-TDP type A, type B and type C. The SNP-level analyses were performed using PLINK v1.90b6.5 64-bit (13 Sep 2018) [73]. Meta-analyses of the discovery and replication results were performed under a fixed-effects model. The I^2 heterogeneity statistics is provided to evaluate the degree of heterogeneity of the effects in the discovery and replication stages.

Gene-level analysis of rare variants

Association of rare variants with the patient/control status was assessed using an unweighted burden test implemented using the SKAT_1.2.1 R package [98]. For the rare-variant analyses, multi-allelic markers were split into multiple "variants" or variables (i.e., multiple rows in the genotype file), with a particular alternate allele being counted for each variable, and with genotypes corresponding to other alternate alleles being set to 0. Thus, each row in the data file represents a count of a particular alternate allele and is only missing when no alleles were called. Only VQSR pass variants with call rate > 90%, ED ≤ 4, and MAF < 0.01 in either patients or controls were included in these rare-variant gene-based analyses. Two sets of analyses were performed: The first included only frameshift (insertion/deletion/block substitution), stopgain, stoploss and splicing SNVs (jointly defined as loss-of-function (LOF) variants), while the second included all variants captured in the first analysis as well as non-synonymous SNVs and non-frameshift indels or block substitutions that were predicted to be probably damaging by Polyphen 2 and deleterious by SIFT [1, 62]. Sex and the first four PCs were used as covariates in the model. As with the common SNP GWAS, analyses were performed with all FTLD-TDP patients, followed by exploratory analyses in pathological FTLD-TDP strata. Because adjustment for PCs in extremely rare variants might lead to spurious associations due to the rarity of mutation carriers, *p* values are provided with and without the incorporation of PCs in the models. Finally, for the rare-variant analysis in *DPP6,* we included all missense variants and LOF variants passing quality control and with a MAF < 0.01 in either patients or controls, and performed a SKAT test as implemented in the SKAT R package allowing bidirectionality of the effect of variants. The association was assessed with and without adjustment for the associated common SNPs in *DPP6* (rs4726389 and rs118113626). Exome-wide significance was defined as a *p* value < 2.5e − 06 (Bonferroni correction for 20,000 genes).

Gene prioritization

All genes with nominal significance identified through burden test with rare LOF mutations or coding variants predicted to be pathogenic by Polyphen2 and SIFT prediction software were subject to a gene ontology (biological processing) and KEGG pathway analysis using Webgestalt [94, 103]. In addition, for all genes where at least 3 such variants were identified in FTLD-TDP patients and none in controls, a similarity analysis using the ToppGene database was performed [11]. As training set, we used the following genes: *C9orf72*, *GRN*, *TBK1*, *OPTN*, *VCP*, *TARDBP*, *CHCHD10*, *SQSTM1*, *UBQLN2*, *hnRNPA1*, *hnRNPA2B1*, *CSF1R*, *FUS*, *CHMP2B*, *LRRK2* and *TIA1*. The default training parameters were used as follows: Gene ontology molecular function, biological process and cellular component; human and mouse phenotype; pathway (BIOCYC, KEGG, Pathway Interaction Database, REACTOME, GenMAPP, MSigDB C2 BIOCARTA (v6.0), PantherDB, Panther Ontology, SMPDB); PubMed and Disease. For each gene , false discovery rate qvalues are reported.

Results

Frequency of known gene mutations within the International FTLD-TDP WGS Consortium

Through collaborative efforts across North America, Europe and Australia, we established the International FTLD-TDP WGS Consortium and identified 1154 unrelated patients with a pathologically confirmed diagnosis of FTLD-TDP and a source of DNA available for basic genetic characterization (Table 1). Analyses of common known genetic causes of FTLD-TDP revealed *C9orf72* repeat expansions in 25.5% and *GRN* mutations in 13.8% of Caucasian patients, together explaining the disease in nearly 40% of our Caucasian FTLD-TDP cohort. *TBK1* and other rare gene mutations accounted for an additional 0.9% and 1.2% of Caucasian patients, respectively, with the caveat that these genes were only analyzed in a subset of patients. In the non-Caucasian population, *GRN* mutations were the most frequent, explaining 20.0% of patients, compared to only 10.0% of FTLD-TDP patients with the *C9orf72* repeat expansion.

To identify genetic factors contributing to the disease in Caucasian FTLD-TDP patients without a known gene mutation, we next performed WGS on 554 patients with sufficient DNA quality and quantity available. A total of 982 individuals from the Mayo Clinic Biobank Study underwent WGS at the same time (Table 2). For each patient,

pathological FTLD-TDP subtyping was available based on TDP-43 immunostaining. FTLD-TDP type B was most common ($n=199$), followed by FTLD-TDP type A ($n=171$) and C ($n=161$). FTLD-TDP type D (*VCP* gene negative) was observed in 4 patients and in 19 patients, the subtyping was ambiguous. The distribution of ages at onset, ages at death and survival after onset was significantly different between the FTLD-TDP subtypes (Kruskal–Wallis test p value$_{\text{age at onset}} = 6.2e-10$; p value$_{\text{age at death}} = 2.0e-14$; p value$_{\text{survival after onset}} < 2.2e-16$, Fig. 1, Table 3). In particular, FTLD-TDP type-A patients were the oldest at onset with a median age of 68.0 years ($IQR_{TDPA} = 59.0–75.8$), which was significantly different from FTLD-TDP type-B and type-C patients ($AAO_{TDPB} = 62.0$, $IQR_{TDPB} = 55.0–69.0$, p value $= 5.3e-07$; $AAO_{TDPC} = 60.8$, $IQR_{TDPC} = 55.8–65.4$, p value $= 4.9e-09$). FTLD-TDP type-B patients died significantly younger ($AAD_{TDPB} = 67.0$, $IQR_{TDPB} = 60.0–74.0$) as compared to FTLD-TDP type-A patients ($AAD_{TDPA} = 78.0$, $IQR_{TDPA} = 67.0–85.0$, p value $= 8.4e-15$) and FTLD-TDP type-C patients ($AAO_{TDPC} = 72.0$, $IQR_{TDPC} = 66.7–76.0$, p value $= 4.9e-05$) and FTLD-TDP type-C patients had the longest survival after onset with a median survival of 11.0 years ($IQR_{TDPC} = 8.1–13.2$) as compared to 7.2 years ($IQR_{TDPA} = 4.0–11.0$, p value $= 9.0e-08$) in FTLD-TDP type A and 3.8 years ($IQR_{TDPB} = 2.0–6.0$, p value $= 2.7e-35$) in FTLD-TDP type B.

After quality control, 517 FTLD-TDP patients and 838 controls free of neurodegenerative disorders were retained and included in genetic studies. An average sequencing depth of 40× was achieved for both patients and controls that

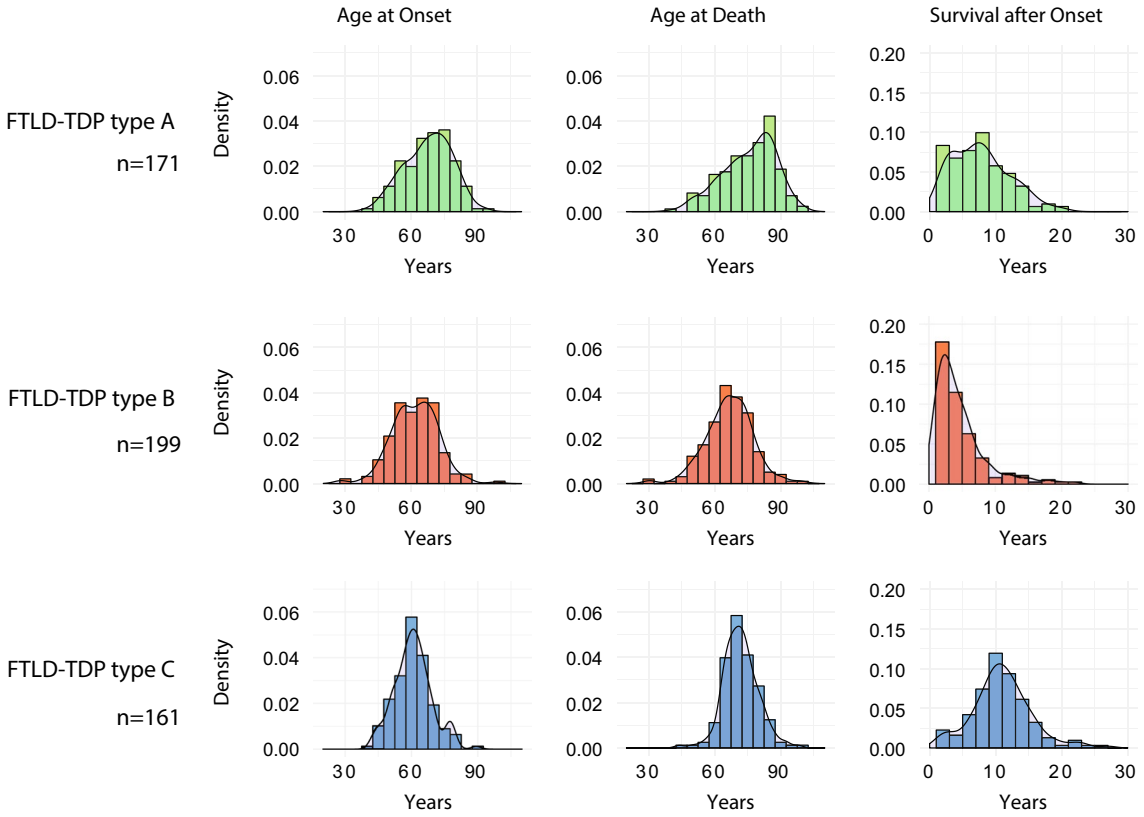

Fig. 1 Age distributions in each FTLD-TDP pathological subtype. Age at onset, age at death and survival after onset are represented as histogram per FTLD-TDP pathological subtype. A density curve is superimposed to the histograms

Table 3 Demographics of FTLD-TDP patients included in the whole-genome sequencing

Group	Age at onset (IQR)	Age at death (IQR)	Survival after onset (IQR)
FTLD-TDP type A ($n=171$)	68.0 (59.0–75.8)	78.0 (67.0–85.0)	7.2 (4.0–11.0)
FTLD-TDP type B ($n=199$)	62.0 (55.0–69.0)	67.0 (60.0–74.0)	3.8 (2.0–6.0)
FTLD-TDP type C ($n=161$)	60.8 (55.8–65.4)	72.0 (66.7–76.0)	11.0 (8.1–13.2)

Median age at onset, age at death and age at last healthy visit of patients are presented (in years). IQR: interquartile range

passed quality controls. To further characterize the presence of known gene mutations within our FTLD-TDP cohort, we first queried the whole-genome dataset for variants observed in FTLD-TDP patients with a minor allele frequency < 0.1% in the EXAC database and absent from our control dataset in the following genes: *GRN*, *TBK1*, *OPTN*, *VCP*, *TARDBP*, *CHCHD10*, *SQSTM1*, *UBQLN2*, *hnRNPA1*, *hnRNPA2B1*, *CSF1R*, *FUS*, *CHMP2B, LRRK2*, and *TIA1*. This led to the identification of LOF mutations in *TBK1* in 7 additional FTLD-TDP patients (p $value_{burden} = 5.15e-03$). Together with the 10 *TBK1* carriers that were already known at the initiation of the International FTLD-TDP WGS Consortium, this brings the total to 17 *TBK1* mutation carriers versus none in controls. We also detected two variants in *OPTN*, one variant in *GRN* and one variant in *CHMP2B*, each of which was defined by the American College of Medical Genetics and Genomics (ACMG) as pathogenic (Table 4, Online Resource 2). Of note, the pathogenic *GRN* variant was a splicing variant c.708 + 6_ + 9delTGAG which had been missed due to its position near the 3′ splice site of exon 7 [6]. By adding these newly identified pathogenic variants to the overall cohort, *C9orf72* repeat expansions explained 25.5% of our Caucasian FTLD-TDP cohort, 13.9% of the patients carried a *GRN* mutation, 1.5% carried a *TBK1* mutation and 1.4% carried a mutation in another known disease gene (**suppl. table 1 Online Resource 1**). Conversely, 57.7% of Caucasian FTLD-TDP patients were not explained by mutations in the known genes.

Identification of common FTLD-TDP genetic risk factors

To identify novel common genetic risk factors for FTLD-TDP, we next performed single variant genome-wide association for the 7,083,292 common variants (MAF > 0.01 in either FTLD-TDP patients or controls) that passed quality control in the 517 FTLD-TDP patients and 838 controls. Genomic inflation was moderate ($\lambda = 1.05$). Logistic regression adjusting for sex and first four PCs identified one genome-wide significant locus at chromosome 7q36.2. The signal was driven by two variants: rs4726389 and rs118113626 located in the *DPP6* intron 1 region (Table 5, Fig. 2; $p = 4.63e-08$, OR = 2.453; $p = 4.88e-08$, OR = 2.481, respectively). Both variants at the *DPP6* locus were in linkage disequilibrium ($r^2 = 0.77$ and $D' = 0.88$) and conditional analysis on rs4726389 abolished the significant association of rs118113626. No additional common variants were detected with an $r^2 > 0.5$ at the 7q36.2 locus. Variants rs4726389 and rs118113626 were not reported as expression quantitative trait loci (eQTL) in public databases and rs4726389 had a Regulomedb score of 6 suggesting minor effect on regulatory elements. Moreover, analysis of *DPP6* mRNA expression in a custom RNAseq dataset of frontal

Table 4 Pathogenic variants identified by whole-genome sequencing

Gene name	Variant category	Variant cDNA	Variant Protein	CADD score	ExAC NFE	Sex	Age at Death	Age at Onset	TDP-43 Type	Publications
CHMP2B	Nonsynonymous SNV	NM_014043:c.A618T	p.Q206H	23.9	1.51E−05	F	71	62	C	[15, 69]
GRN	Splice	NM_002087:c.708 + 6_ + 9delTGAG		.	.	M	72	62	A	
OPTN	Frameshift insertion	NM_001008212:c.381_382insAG	p.D127 fs	24.3	2.00E−04	M	70	62.2	A	
OPTN	Stopgain	NM_001008212:c.C703T	p.Q235×	39	.	M	70	64.3	A	[71]
TBK1	Stopgain	NM_013254:c.C349T	p.R117×	39	.	M	72	68	A	[71, 89]
TBK1	Stopgain	NM_013254:c.C1330T	p.R444×	45	1.51E−05	M	60	52	B	[85]
TBK1	Frameshift deletion	NM_013254:c.1328_1331del	p.I443 fs	35	.	M	75	66	A	
TBK1	Stopgain	NM_013254:c.C379T	p.R127×	38	.	F	75	68	A	[89]
TBK1	Stopgain	NM_013254:c.1272delT	p.Y424×	25.8	.	F	54	50	B	
TBK1	Frameshift deletion	NM_013254:c.1886_1889del	p.Q629 fs	35	.	F	78	68	A	
TBK1	Splice	NM_013254:c.992 + 1G > A		24.5	.	M	71	68	B	[89]

Pathogenic variants according to the ACMG criteria are presented along with their predicted pathogenicity (CADD score) and frequency in ExAC non-Finnish European (ExAC NFE). Phenotypic data are presented for each FTLD-TDP carrier and includes sex, age at death, age at onset and the TDP-43 pathological subtype

Table 5 Associations within the discovery, replication and meta-analysis stages for loci identified in the FTLD-TDP patients versus control analysis

SNP ID	Position	Major/minor allele	Locus name	Discovery stage			Replication stage			Meta-analysis		
				MAF in controls/patients	OR (95% CI)	*p* value	controls/patients	OR (95% CI)	*p* value	OR	*p* value	I^2
rs61831315	chr1:186126654	A/G	*HMCN1*	0.05/0.02	0.31 (0.18–0.51)	4.28E−06	0.05/0.06	1.07 (0.60–1.92)	8.13E−01	0.52	9.06E−04	90.17
rs61707463	chr4:169787358	A/G	*C4orf27*	0.02/0.05	3.58 (2.13–6.03)	1.60E−06	0/0	NA	NA	NA	NA	NA
rs11132244	chr4:184422579	A/G	*IRF2*	0.3/0.23	0.64 (0.53–0.78)	9.17E−06	0.27/0.3	1.14 (0.84–1.55)	3.93E−01	0.76	1.06E−03	89.67
rs17219281	chr6:32707868	G/A	*HLA-DQA2*	0.06/0.11	2.06 (1.52–2.79)	3.19E−06	0.07/0.13	1.84 (1.24–2.74)	2.58E−03	1.98	3.22E−08	0
rs6463679	chr7:7305371	G/A	*LOC101927354*	0.34/0.42	1.49 (1.26–1.77)	4.39E−06	0.36/0.41	1.23 (0.93–1.63)	1.43E−01	1.42	2.81E−06	23.39
rs10267171	chr7:110723284	T/C	*IMMP2L*	0.19/0.25	1.61 (1.31–1.98)	6.53E−06	0.2/0.16	0.76 (0.53–1.1)	1.41E−01	1.34	1.34E−03	91.82
rs118113626	chr7:154194746	C/T	*DPP6*	0.05/0.10	2.48 (1.79–3.44)	4.88E−08	0.07/0.09	1.51 (0.94–2.43)	8.91E−02	2.12	4.82E−08	64.89
rs4726389	chr7:154225769	G/A	*DPP6*	0.05/0.10	2.45 (1.78–3.39)	4.63E−08	0.07/0.08	1.27 (0.77–2.08)	3.44E−01	2.02	3.50E−07	79.20
rs13283101	chr9:135082911	G/A	*OLFM1*	0.12/0.20	1.74 (1.38–2.20)	3.30E−06	0.15/0.16	1.01 (0.70–1.45)	9.73E−01	1.49	8.06E−05	83.56
rs12425381	chr12:15176736	C/G	*RERG*	0.24/0.17	0.65 (0.53–0.81)	6.78E−05	0.18/0.13	0.69 (0.39–1.24)	2.14E−01	0.66	3.08E−05	0
rs4240777	chr15:85946519	C/G	*MIR548AP*	0.31/0.40	1.51 (1.27–1.81)	4.97E−06	0.37/0.41	1.16 (0.88–1.53)	3.02E−01	1.40	1.04E−05	59.59
rs12973192	chr19:17642430	C/G	*UNC13A*	0.37/0.45	1.48 (1.25–1.75)	3.44E−06	0.34/0.44	1.57 (1.20–2.04)	9.22E−04	1.5	1.27E−08	0

Each locus is presented with the variants followed up in the replication along with their position, the closest gene (Locus Name), the minor allele frequency in controls and patients (MAF controls/patients), its odds ratio (OR) and *p* value

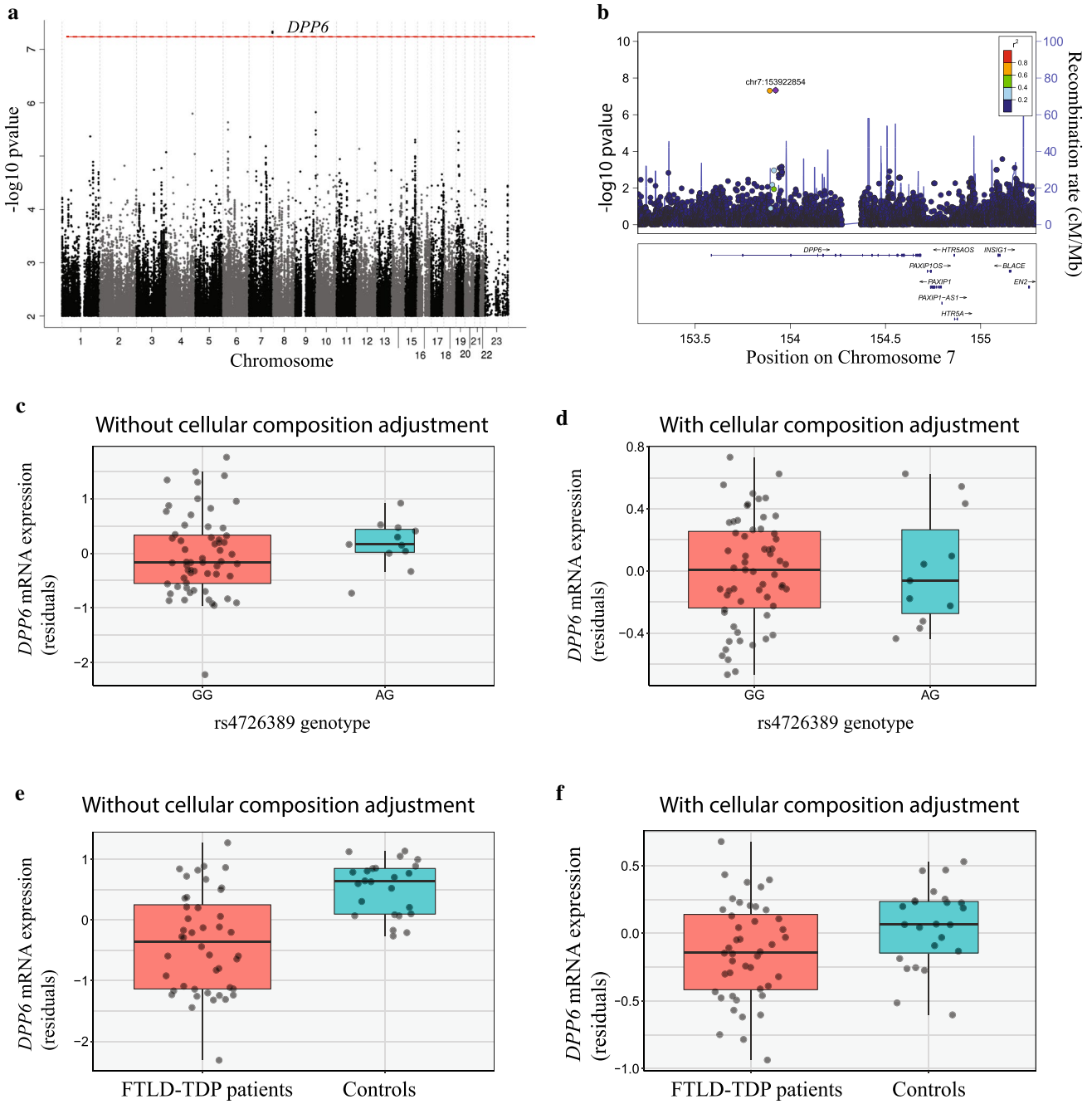

Fig. 2 Common variant whole-genome sequencing association study and *DPP6* locus. **a** Manhattan plot of the FTLD-TDP patients versus control association study. The red-dotted line represents the genome-wide significance level ($p = 5e-08$). **b** Regional association (locus zoom) plot of the *DPP6* locus. Each dot represents a genotyped variant. The purple dot is the most significant variant (rs4726389) among variants in the region. Dots are colored from red to blue according to their r^2 value, showing their degree of linkage disequilibrium with rs4726389 (grey indicates an r^2 of zero). The light blue line shows the estimated recombination rate. **c** *DPP6* mRNA expression levels in function of the rs4726389 genotypes without correction for cellular composition in custom RNAseq frontal cortex dataset. **d** *DPP6* mRNA expression levels in function of the rs4726389 genotypes with correction for cellular composition in custom RNAseq frontal cortex dataset. **e** Differential *DPP6* mRNA expression levels in FTLD-TDP patients and controls without correction for cellular composition. **f** Differential *DPP6* mRNA expression levels in FTLD-TDP patients and controls with correction for cellular composition

cortex tissue samples of FTLD-TDP patients ($n = 68$) did not show an effect of rs4726389 on *DPP6* mRNA expression (p value = 0.88 after FDR correction, fold change = 1.01; Fig. 2). Compared to control tissue samples, we did observe a decrease in *DPP6* mRNA expression in FTLD-TDP patients; however, after correction for cell-type composition,

this association was no longer significant (p value = 0.89 after FDR correction, Fig. 2). By investigating the presence of rare variants in *DPP6* in our dataset, we further identified one LOF variant in our FTLD-TDP patients: the splice variant c.1345 + 1G > T (cDNA position is provided according to NM_130797), whereas LOF variants were not observed in our control cohort. The LOF variant reduced cortex mRNA expression of *DPP6* by 41% and cDNA sequencing suggested degradation of the mutant allele by nonsense-mediated decay (suppl. Figure 1 Online Resource 1). We also identified 26 *DPP6* non-synonymous variants with a MAF less than 1% in either patients or controls. A SKAT test including the two LOF variants and the 26 missense variants resulted in a trend towards association of *DPP6* rare damaging variants with FTLD-TDP but failed to reach significance (p value = 0.07). After adjustment for the top common SNPs, this result did not change substantially suggesting the *DPP6* common variant and rare variant associations with FTLD-TDP are independent from one another.

In addition to the *DPP6* locus, 12 suggestive loci with a p value < 1e − 05 were identified (Table 5). Of the 13 loci, 11 were successfully followed up in an independent replication cohort of newly ascertained FTLD-TDP patients (n = 119) and controls (249 pathologically confirmed normal controls and 1404 clinical controls). A meta-analysis combining the discovery and the replication stages resulted in three loci with genome-wide significance (Table 5). Rs118113626 at the *DPP6* locus remained genome-wide significant, despite some heterogeneity between the two stages. The strongest signal, however, was found at chromosome 19p13.11 at the *UNC13A* locus, with top SNP rs12973192 (p value = 1.27e − 08, OR = 1.50) followed by rs17219281 on chromosome 6p21.32 at the *HLA-DQA2* locus (p value = 3.22e − 08, OR = 1.98). According to the GTex database, rs17219281 is reported as an eQTL for *HLA-DQB2* and *HLA-DQA2* with the most significant association found with their expression in cortex for *HLA-DQB2* (p value = 6.2e − 07) and in amygdala for *HLA-DQA2* (p value = 2.7e − 03); the rare allele consistently increasing *HLA-DQB2* and *HLA-DQA2* gene expression.

In exploratory analysis, we next performed genome-wide association analyses within each FTLD-TDP strata (FTLD-TDP type A, B and C). Loci which showed suggestive association (p value < 1e − 05) in at least one of the strata are shown in suppl. Table 3 (Online Resource 1). Interestingly, rs12973192 in *UNC13A* reached genome-wide significance within FTLD-TDP type B (p value = 4.67e − 08, OR = 1.95), with virtually no association of rs12973192 with FTLD-TDP type A and C (p $\text{value}_{\text{TDPA}}$ = 1.90e − 02, OR = 1.35; p $\text{value}_{\text{TDPC}}$ = 4.94e − 01, OR = 1.10). In contrast, within FTLP-TDP type-A patients, the *GRN* locus on chromosome 17 showed most significance. While the additive model resulted in a suggestive p value of 1.69e − 07 at this locus in FTLD-TDP type A (rs708384), further investigation under different modes of inheritance showed a much stronger and genome-wide significant signal using a recessive model with most significance at rs5848 located in the 3′untranslated region of *GRN* (p value = 4.99e − 12; OR = 5.16). No genome-wide significant associations were found in FTLD-TDP type C.

Finally, KEGG pathway enrichment analysis including all suggestive loci in either the overall FTLD-TDP cohort or pathological strata (suppl. Table 2 Online Resource 1) highlighted a significant overrepresentation of the inflammatory pathway (p $\text{value}_{\text{FDR}}$ = 2.79e − 02) represented by the presence of the *HLA* locus, *MAF* and *TLR4* genes.

Identification of rare FTLD-TDP genetic risk factors

To identify genes carrying rare FTLD-TDP risk variants, we first focused only on genes that carried LOF variants. Gene-burden analyses including only these variants did not show exome-wide significant association (Online Resource 3) and gene ontology and pathway enrichment analyses on all nominally significant genes revealed no particular enrichment in biological processes (data not shown). We then focused on 61 genes in which we observed LOF variants in at least 3 patients and none in controls. *TBK1* showed the most LOF mutation carriers (n = 7, as discussed above). Prioritization of the remaining 60 genes based on similarities with known FTLD-TDP genes using ToppGene identified *TRIM21* as the top gene based on its functional role within the *TBK1*-regulated innate immunity pathway (three LOF carriers, p $\text{value}_{\text{ToppGene}}$ = 1.97e − 04 after FDR correction, Online Resource 4). Two additional genes which are known to function in the same pathway showed significant similarity to known FTLD-TDP genes according to ToppGene: *IRF-7* (three LOF carriers, p $\text{value}_{\text{ToppGene}}$ = 8.68e − 04 after FDR correction) and *DHX58* (four LOF carriers, p $\text{value}_{\text{ToppGene}}$ = 1.43e − 02 after FDR correction) (Online Resource 5). Interestingly, manual inspection of the LOF variants observed in our WGS cohort also revealed one FTLD-TDP patient each with LOF variants in *IRF8*, *IRF3* and *NOD2* and no LOF variants in controls in these genes, further highlighting the importance of the *TBK1*-regulated innate immunity pathway in FTLD-TDP (suppl. figure 2 Online Resource 1). As a second analysis, we broadened our filtering criteria allowing variants predicted to be pathogenic by two prediction algorithms (Polyphen-2 and SIFT) to be added to the LOF variants (Online Resource 3). This resulted in one exome-wide significant gene in the burden analysis (*OSBPL3)*; however, this association did not remain significant when PCs were excluded from the model (p value = 7.61e − 07, p $\text{value}_{\text{noPC}}$ = 2.24e − 04). Again, gene ontology and pathway analyses on the nominally significant genes failed to detect enrichment in biological processes

(data not shown). When we selected genes which carried LOF variants and coding variants predicted to be pathogenic in at least three patients and no controls, similarity analysis with ToppGene ranked *NPC1* as the gene most closely resembling known FTLD-TDP genes (three variants, p value$_{\text{ToppGene}} = 6.33e-05$ after FDR correction, Online Resource 4).

Discussion

The significant heterogeneity in clinical and pathological presentations among FTLD patients and the strong correlations between known gene mutations and pathological FTLD subgroups prompted our initiative to establish the international FTLD-TDP whole-genome sequencing consortium. This allowed us to provide a comprehensive overview of the most common known genetic causes of FTLD-TDP and it formed the basis of an unbiased genome-wide association study which implicated both common variants at the *DPP6*, *UNC13A* and *HLA-DQA2* genomic loci and rare LOF variants in genes involved in the TBK1-immunity pathway in the genetic etiology of FTLD-TDP. The careful pathological classification of each patient included in the WGS study into an FTLD-TDP pathological subtype, also confirmed rs5848 located in the 3′UTR of *GRN* as a major risk factor for FTLD-TDP, specifically in FTLD-TDP type A.

Focusing on the known genes, combined analysis of 1151 FTLD-TDP patients across 23 international sites clearly established the *C9orf72* repeat expansion as the most common known genetic cause of FTLD-TDP in Caucasian populations, explaining 25.5% of patients. We observed a wide range of *C9orf72* mutation frequencies across sites (from 10.3% to 45.5%), which likely reflects the specialized nature of certain clinics and the relative number of FTLD-MND patients that are followed. While we carefully excluded known relatives, the presence of founder effects may have also inflated the *C9orf72* disease frequency in certain populations, as suggested elsewhere [88]. Regardless, the high frequency of *C9orf72* repeat expansions in FTLD-TDP patients underscores the importance of understanding the multiple disease mechanisms associated with this mutation such that effective therapies can be developed for this significant patient subgroup [5]. Interestingly, in our non-Caucasian FTLD-TDP patients, only 10.0% carried a *C9orf72* repeat expansion, compared to 20.0% of patients with a *GRN* mutation. While we cannot draw definitive conclusions due to the small sample size, *GRN* mutations, thus, appear to be the major known genetic cause of FTLD-TDP among non-Caucasian populations.

We next focused on the 57.7% of Caucasian FTLD-TDP patients who remained unexplained after careful analysis for the presence of pathogenic mutations in known genes. WGS was performed on all patients with sufficient DNA quality and quantity available and 517 FTLD-TDP patients and 838 controls were eventually included in unbiased genetic association studies. At the discovery stage, a common variant genome-wide analysis identified the *DPP6* locus at chromosome 7q36 as a novel FTLD-TDP risk locus, with further validation at the meta-analysis stage which included 119 additional FTLD-TDP patients and 1653 controls. DPP6 is a type II transmembrane protein exclusively expressed in neurons [14]. It is a binding partner of the Kv4-containing A-type K+ channels which are important for determining cellular excitability. Based on available studies in mouse and human, one could hypothesize that FTLD-TDP-associated risk variants reduce the amount of functional DPP6: *Dpp6* knockout mice show a reduction of hippocampal glutamatergic synapses and impaired hippocampus-dependent learning behavior and memory [51, 82], *DPP6* LOF mutations in humans have been associated with neurodevelopmental disorders [49] and autoantibodies against DPP6 were found to be the cause of a multifocal neurologic disorder of the central and autonomic nervous system [7, 35, 84]. The identification of one *DPP6* LOF mutation in our FTLD-TDP patient cohort is further in line with a LOF disease-risk mechanism. However, no effect of our top variants (rs4726389 and rs118113626) on brain *DPP6* mRNA expression levels could be detected, using either publically available data or a custom-derived frontal cortex RNAseq dataset. Given that these measures were obtained from relatively small numbers of post-mortem tissue samples, using bulk RNAseq, these findings do not exclude an effect of these variants on DPP6 expression in (specific) neuronal populations. In addition, while our lead SNPs are located in intron 1 of *DPP6*, we cannot rule out an effect on more distantly located genes. It also remains possible that the observed risk variants tag a rarer functional variant, only present in a subset of patients, which would have hampered our ability to detect an effect. Such functional variant(s) may well be a complex rearrangement given that the chromosome 7q36 region is enriched with low copy repeats which increase the chance of recombination and chromosomal rearrangements, as described [25]. Long-range next-generation sequencing technologies would be needed to test this hypothesis in future studies. In fact, in an independent study, paired-end and long-reads Nanopore WGS in a previously unresolved autosomal dominant early-onset dementia family linked to 7q36 led to the identification of a large ~ 4 Mb chromosomal inversion disrupting DPP6, further implicating loss of DPP6 expression and/or function in early-onset dementia (Cacace et al., submitted, [10]). Finally, while the *DPP6* locus has been previously associated with ALS in some but not all studies [13, 16, 18, 22, 29, 64, 72, 90, 92], the top ALS-associated variant (rs10260404)

is not in LD with our top SNPs (rs4726389 and rs10260404: $r^2 = 0.004$).

A meta-analysis of the discovery and replication stages revealed two additional genome-wide significant loci: *UNC13A* and *HLA*. The *UNC13A* locus signal was driven by rs12973192 which is in strong LD with rs12608932, a variant associated with ALS [91]. In fact, a meta-analysis of ALS and an earlier performed FTLD-TDP GWAS reached genome-wide association at the *UNC13A* locus [24], but failed to reach significance in the FTLD-TDP cohort alone [24, 86]. More recently, *UNC13A* variant rs12608932 was shown to act as a phenotypic modifier in ALS patients by increasing the risk for frontotemporal cortical atrophy and impaired cognitive performance, reminiscent of an FTLD clinical presentation [70]. We also detected a genome-wide significant signal at the *HLA* locus on chromosome 6p21.32 led by rs17219281 which is located upstream of the *HLA-DQA2* and *HLA-DQB2* genes and has been reported as an eQTL with the rare allele (associated with FTLD-TDP risk) robustly increasing the expression of *HLA-DQA2* and *HLA-DQB2* transcripts in several brain regions. Even though most *HLA* genes are highly polymorphic, the *HLA-DQA2* and *HLA-DQB2* genes are poorly polymorphic; yet their biological function has not been well characterized [46]. Importantly, the *HLA* locus has previously been implicated in other neurodegenerative disorders including Alzheimer's and Parkinson's disease (PD) [34, 43, 61]. Moreover, a large GWAS identified rs9268877 at the *HLA-DRA* locus on 6p21.32 as a risk factor for clinical FTLD [27] with subsequent studies emphasizing a possible genetic overlap between FTLD and PD through rs9268877 [27, 28]. Our FTLD-TDP-associated lead SNP (rs17219281) is not in LD with rs9268877 ($r^2 = 0.03$) and in contrast to our lead SNP, the FTLD and PD-associated risk allele of rs9268877 was associated with reduced expression of *HLA-DQA2* transcripts [28]. Therefore, even though we identified association of FTLD-TDP with a known FTLD risk locus, the specific risk variant(s) and the associated disease mechanisms may vary across diseases and give rise to distinct neuropathologies. It will likely require the use of dedicated bioinformatic pipelines designed to analyze the high complexity of the HLA region to further clarify this issue.

The requirement of TDP-43 immunohistochemistry and pathological FTLD-TDP subtyping for all patients included in the WGS provided a level of quality control in terms of patient inclusion above and beyond that of previous studies. It also provided the first opportunity to test the hypothesis that different genetic factors influence disease risk in distinct FTLD-TDP pathological strata. Excitingly, using only 184 FTLD-TDP type B patients, we identified genome-wide significant association with variants in *UNC13A*, illustrating the power of our approach and confirming the overlap between ALS and FTLD-TDP type B in particular. In patients with FTLD-TDP type A, a more than fivefold increased risk was detected for patients homozygous for the rare T-allele of rs5848 located in a microRNA-binding site within the *GRN* 3′UTR [74] (p value$_{REC} = 4.99e-12$; OR = 5.16), whereas no risk was observed in FTLD-TDP type-B (p value$_{REC} = 2.04e-2$; OR = 1.44) and type-C (p value$_{REC} = 8.94e-1$; OR = 1.05) patients. Pathological heterogeneity within previously studied patient cohorts (e.g., variable proportions of FTLD-TDP type-A patients) likely contributed to the discrepant reports on the role of rs5848 in FTLD published in the last decade [12, 74, 76, 81]. Importantly, however, we previously showed that the r5848 risk allele is associated with reduced GRN expression in cerebellar tissue samples to a level intermediate between *GRN* mutation carriers and controls [74] and similar effects of rs5848 on expression were reported in plasma and cerebrospinal fluid [37, 63]. These findings suggest that reduced GRN levels (resulting from rs5848) may contribute to FTLD-TDP type-A disease risk in at least a subset of the patients without *GRN* LOF mutations. This would expand the overall contribution of *GRN* dysfunction to FTLD-TDP with likely significant implications once *GRN*-related therapies become available. For FTLD-TDP type C, best known for its lack of a positive family history in most patients, we did not identify any genome-wide significant risk factors; however, this may have been a result of a lack of power (only 143 FTLD-TDP type C in association study).

Finally, our study also sheds new light on TBK1 and the role of the innate immune signaling in FTLD. Neuroinflammation and immunity have previously been reported in the context of FTLD, and the idea that immune dysfunction may contribute to FTLD risk is not new. Microglial activation is a pathological hallmark of patients with FTLD [44, 67, 83] and a key feature of genetic FTLD mouse models [41, 53, 80, 100] and both *GRN* and *C9orf72* have been extensively linked to neuroinflammation and microglial activation [42, 56, 66, 100]. Genetic overlap between immune-mediated diseases and clinical FTLD was recently reported [8] and independent studies found an increased prevalence of autoimmune conditions in patients with *GRN* and *C9orf72* mutations, and in clinical FTLD patients predicted to have an underlying FTLD-TDP pathology (svPPA and FTLD-MND) [59, 60]. In our study, we confirmed the importance of *TBK1* by establishing it as the third most common genetic cause of FTLD-TDP, with LOF variants in 1.5% of Caucasian FTLD-TDP patients. Moreover, even though we did not have statistical power to detect exome-wide significant association in our rare-variant burden analysis, prioritization of genes with an excess of LOF variants in FTLD-TDP patients ($n \geq 3$) versus controls ($n = 0$) detected several other genes involved in the regulation of inflammation and immunity through TBK1 (*TRIM21*, *DHX58*, *IRF7*, *IRF3*, *IRF8* and *NOD2*). Segregation data as well as independent replication are necessary to infer a causal or risk effect of such

LOF variants. *TBK1* encodes a protein kinase involved in regulation of the immune response, autophagy and inflammation [36]. In the innate immune signaling pathway, TBK1 can be activated through multiple pathways including double stranded (ds)RNA (TLR3-TRIF), lipopolysaccharides (TLR4-TRIF), viral RNA (RIG-I-MAVs) and dsDNA (cGAS-STING) resulting in the phosphorylation and activation of IRF3/IRF7 (suppl. figure 2 Online Resource 1) [48, 52, 65]. *TBK1* mutations observed in ALS and FTLD-TDP patients were previously shown to reduce the activation of IRF3 [20, 30, 39, 85], and our observation of LOF variants in *IRF3*, *IRF7* and *IRF8* in FTLD-TDP patients, thus, points to alternative genetic insults that may have similar consequences. TRIM21, with LOF variants in 3 FTLD-TDP patients, also positively regulates innate immunity by facilitating the recruitment of TBK1 to MAVS through the regulation of MAVS polyubiquitination [99]. DHX58 (mutated in 4 FTLD-TDP patients) was originally thought to be a negative regulator of the RIG-I-like receptor family [40, 77, 78, 101]; however, more recent work has shown the importance of DHX58 in the enhancement of MDA5-mediated antiviral signaling in vivo [79, 93]. In fact, studies in *Dhx58* knock-out mice found that Dhx58 was essential for type I IFN production in response to picornaviridae infection [79]. In combination, our findings suggest a critical role for impaired interferon production in FTLD-TDP; however, TBK1 is also well known for its role in the autophagy pathway through interactions with OPTN and SQSTM1, two other proteins implicated in FTLD-TDP etiology [2]. Future studies should, therefore, decipher the respective roles of IFN signaling and autophagy in TBK1-related FTLD-TDP and the possible crosstalk between these two pathways [79].

Our study also has some limitations. Since we only recruited 20 non-Caucasian FTLD-TDP patients, the *GRN* and *C9orf72* mutation frequencies in this cohort may be unreliable and novel gene discovery was not possible. Second, while we included the analyses of both common and rare variants, this study only focused on highly selected rare variants and we did not analyze copy number and structural variants. Further studies are, therefore, necessary to provide a full overview of the genetic factors contributing to FTLD-TDP. Third, the relatively small sample size of our discovery and replication cohorts may have resulted in a lack of statistical power to detect weak genetic associations with disease risk. The use of clinical FTLD cohorts, enriched for patients with certain clinical FTLD subtypes, may be one possible avenue for future replication studies; however, while some genetic risk factors will benefit from such approach, some true genetic risk factors may fail to replicate due to an increased heterogeneity of underlying pathologies.

In conclusion, our analysis of the largest cohort of pathologically characterized patients with FTLD-TDP, in which mutations in the known causal genes *GRN* and *C9orf72* were excluded, identified three genomic loci harboring common FTLD-TDP risk variants: *DPP6*, *UNC13A* and *HLA-DQA2*, and an excess of rare LOF variants in the TBK1-related innate immunity pathway in FTLD-TDP patients as compared to controls. Future work will focus on the identification of functional variants and their associated disease mechanism at each of the associated loci; however, we nominate *DPP6* with its modulating effect on K-channel activation as a possible novel FTLD-TDP risk gene and we strongly implicate the immune pathway in FTLD-TDP pathogenesis.

Acknowledgements We thank all colleagues and staff at the participating centres for their help with recruitment of patients. Specifically, we thank Drs. Etty P. Cortes, Allan Levey, James Lah, Chad Hales, William Hu, Inger Nennesmo, Håkan Thonberg, Huei-Hsin Chiang, Ivy and Jeffrey Metcalf, David Lacomis, Nick Fox, Martin Rossor, Jason Warren, Michael DeTure. We also thank Virginia Phillips, Linda Rousseau, Monica Casey-Castanedes, Pheth Sengdy, Alice Fok, Charlotte Forsell, Anna-Karin Lindström, Veronika Kaltenbrunn, Brigitte Kraft, Vanessa Boll, Chan Foong. This work was supported by the NIH from NIA: P50 AG008702 (LSH, J-PV, EPC); P50 AG025688 (MG and JDG); P30 AG010133 (BG, MF, JG, EDH); P30 AG013854 (EB, MM, SW,CG); R01 AG051848 and P50 AG005131 (RAR); P01 AG017586, P30 AG01024, U01 AG052943 (VVD, MG, DJI, EBL, JQT, ES); P50 AG005133 (JK, OLL), P30 AG012300 (CLWIII, BME); P50 AG005681, P01 AG003991 and U01 AG058922 (NJC, CC); P30 AG019610 (EMR); UO1 AG006786 and RO1 AG041797 (BFB); R01 AG037491 (KAJ); P50 AG016574 (RCP, BFB, RR, DWD, DSK, NRG-R); U01 AG046139 (NE-T); the Longitudinal Evaluation of Familial Frontotemporal Dementia Subjects U01 AG 045390 (BFB); K01 AG049152 (JSY). In addition part of the project was supported by the NIH from NIDCD: R01 DC008552 (RAR); and by the VA: I01 BX003040 (RAR). This research was supported by the University of Pittsburgh Brain Institute (JK, OLL); Carl B. and Florence E. King Foundation, McCune Foundation, Winspear Family Center for Research on the Neuropathology of Alzheimer Disease (CLWIII, BME); Arizona Department of Health Services contract #211002, Arizona Biomedical Research Commission contracts #4001, #0011, #05-901, #1001, the Michael J. Fox Foundation for Parkinson's Research, Mayo Clinic Foundation and Sun Health Foundation (TGB). This work was supported by the NIH from NINDS: R35 NS097261 (RR); UH3/UG3 NS103870 (RR); U54 NS092089 (BFB, ALB); P01 NS084974 (DWD); R01 NS080820 (N.E-T); P50 NS072187 (ZKW); R01 NS076837 (EDH), P30 NS055077 (MG), U24 NS072026 (TGB); R01 NS085770 (CG). We thank the Mayo Clinic Center of Individualized Medicine for collection and sequencing of the Mayo Clinic Biobank samples. This work was further supported by grants from the Consortium for Frontotemporal dementia (RR), the Bluefield Project to Cure FTD (RR), the Mayo Clinic Dorothy and Harry T. Mangurian Jr. Lewy Body Dementia Program and the Little Family Foundation (BFB). Whole-genome sequencing was in part funded through the Rainwater Charitable Foundation (JSY). The Columbia University Brain Bank is supported by NIH Grant NIH/NIA P50 AG008702 (ADRC). The brain samples from the Netherlands were obtained from the Netherlands Brain Bank, Netherlands Institute for Neuroscience, Amsterdam (open access: www.brainbank.nl). All material has been collected from donors for or for whom a written informed consent for a brain autopsy and the use of the material and clinical information for research purposes had been obtained by the NBB. Whole-genome sequencing of Dutch samples was supported by the "Gieskes-Strijbis foundation" as project "Semantic dementia unraveled" and through the "2bike4alzheimer" initiative by the "Alzheimer Netherlands foundation" as project

"WE.09-2017-05" (JCvS, HS, JGJvR, MOM). Tissue samples were supplied by the London Neurodegenerative Diseases Brain bank, which receives funding from the Medical Research Council UK and as part of the Brains for Dementia Research programme, jointly funded by Alzheimer's Research UK and Alzheimer's Society (CT, SA-S, AK). JDR is supported by an MRC Clinician Scientist Fellowship (MR/M008525/1), an NIHR Rare Disease Translational Research Collaboration fellowship (BRC149/NS/MH), the Bluefield Project, the MRC UK GENFI Grant (MR/M023664/1), the NIHR UCL/H Biomedical Research Centre, Alzheimer's Research UK and the Alzheimer's Society. SM is an NIHR senior investigator and is funded by the UK Medical Research Council and the NIHR UCL/H Biomedical Research Centre. SP-B was supported by the MRC Grant G0701441. The study was in also supported in part by institutional grants from the DZNE for "DZNE Brain Bank" and "Frontotemporal lobar degeneration: From basic mechanisms and target identification to translational and clinical approaches/Clinical Project" (MNPH, PR, JS-S, MS, JP). The work was also supported by the Hans und Ilse Breuer Foundation, Munich Cluster of Systems Neurology (SyNergy), European Community's Health Seventh Framework Programme under Grant agreement 617198 [DPR-MODELS] (TA, DE, JH, SR). CW was supported by the fortüne program of the University of Tübingen (#2488-0-0). Research was supported by Grants provided by the Swedish research Council (Dnr 521-2010-3134, 529-2014-7504, 2015-02926), Alzheimer Foundation Sweden, Brain Foundation Sweden, Swedish FTD Initiative- Schörling foundation, Swedish Brain Power, Karolinska Institutet doctoral founding, Galma Tjänarinnor, Stohnes Foundation, Dementia Foundation Sweden and the Stockholm County Council (ALF-project). The brain pathology was provided through the Brain Bank at Karolinska Institutet which was financially supported by Karolinska Institutet StratNeuro, Swedish Brain Power, Stockholm County Council core facility funding (CG, LO). This work was also funded through the Canadian Consortium on Neurodegeneration in Aging (ER); in particular from CCNA #137794 (RG-Y, IRM); CIHR Operating Grant #327387 (ECF); #179009 (RG-Y, IRM). GMH, JBK, JRH, OP—The Sydney Brain Bank is funded by Neuroscience Research Australia and the University of New South Wales. The ForeFront Brain and Mind project team a large collaborative research group dedicated to the study of neurodegenerative diseases and funded by the National Health and Medical Research Council of Australia Program Grant (#1132524), Dementia Research Team Grant (#1095127), NeuroSleep Centre of Research Excellence (#1060992), and the ARC Centre of Excellence in Cognition and its Disorders Memory Program (CE10001021). OP is supported by a NHMRC Senior Research Fellowship (#1103258). GMH is supported by a NHMRC Senior Principal Research Fellowship (#1079679).

Compliance with ethical standards

Informed consent Informed consent was obtained from all individual participants included in the study.

References

1. Adzhubei IA, Schmidt S, Peshkin L, Ramensky VE, Gerasimova A, Bork P et al (2010) A method and server for predicting damaging missense mutations. Nat Methods 7:248–249. https://doi.org/10.1038/nmeth0410-248
2. Ahmad L, Zhang SY, Casanova JL, Sancho-Shimizu V (2016) Human TBK1: a gatekeeper of neuroinflammation. Trends Mol Med 22:511–527. https://doi.org/10.1016/j.molmed.2016.04.006
3. Allen M, Wang X, Burgess JD, Watzlawik J, Serie DJ, Younkin CS et al (2018) Conserved brain myelination networks are altered in Alzheimer's and other neurodegenerative diseases. Alzheimers Dement 14:352–366. https://doi.org/10.1016/j.jalz.2017.09.012
4. Baker M, Mackenzie IR, Pickering-Brown SM, Gass J, Rademakers R, Lindholm C et al (2006) Mutations in progranulin cause tau-negative frontotemporal dementia linked to chromosome 17. Nature 442:916–919. https://doi.org/10.1038/nature05016
5. Balendra R, Isaacs AM (2018) C9orf72-mediated ALS and FTD: multiple pathways to disease. Nat Rev Neurol 14:544–558. https://doi.org/10.1038/s41582-018-0047-2
6. Bit-Ivan EN, Suh E, Shim HS, Weintraub S, Hyman BT, Arnold SE et al (2014) A novel GRN mutation (GRN c.708+6_+9delTGAG) in frontotemporal lobar degeneration with TDP-43-positive inclusions: clinicopathologic report of 6 cases. J Neuropathol Exp Neurol 73:467–473. https://doi.org/10.1097/NEN.0000000000000070
7. Boronat A, Gelfand JM, Gresa-Arribas N, Jeong HY, Walsh M, Roberts K et al (2013) Encephalitis and antibodies to dipeptidyl-peptidase-like protein-6, a subunit of Kv4.2 potassium channels. Ann Neurol 73:120–128. https://doi.org/10.1002/ana.23756
8. Broce I, Karch CM, Wen N, Fan CC, Wang Y, Tan CH et al (2018) Immune-related genetic enrichment in frontotemporal dementia: an analysis of genome-wide association studies. PLoS Med 15:e1002487. https://doi.org/10.1371/journal.pmed.1002487
9. Buee L, Delacourte A (1999) Comparative biochemistry of tau in progressive supranuclear palsy, corticobasal degeneration, FTDP-17 and Pick's disease. Brain Pathol 9:681–693
10. Cacace R, Heeman B, Van Mossevelde S, De Roeck A, Hoogmartens J, De Rijk P et al (2018) Loss of *DPP6* in neurodegenerative dementia: a genetic player in the dysfunction of neuronal excitability. Acta Neuropathol **(submitted)**
11. Chen J, Bardes EE, Aronow BJ, Jegga AG (2009) ToppGene Suite for gene list enrichment analysis and candidate gene prioritization. Nucl Acids Res 37:W305–W311. https://doi.org/10.1093/nar/gkp427
12. Chen Y, Li S, Su L, Sheng J, Lv W, Chen G et al (2015) Association of progranulin polymorphism rs5848 with neurodegenerative diseases: a meta-analysis. J Neurol 262:814–822. https://doi.org/10.1007/s00415-014-7630-2
13. Chio A, Schymick JC, Restagno G, Scholz SW, Lombardo F, Lai SL et al (2009) A two-stage genome-wide association study of sporadic amyotrophic lateral sclerosis. Hum Mol Genet 18:1524–1532. https://doi.org/10.1093/hmg/ddp059
14. Clark BD, Kwon E, Maffie J, Jeong HY, Nadal M, Strop P et al (2008) DPP6 localization in brain supports function as a Kv4 channel associated protein. Front Mol Neurosci 1:8. https://doi.org/10.3389/neuro.02.008.2008
15. Cox LE, Ferraiuolo L, Goodall EF, Heath PR, Higginbottom A, Mortiboys H et al (2010) Mutations in CHMP2B in lower motor neuron predominant amyotrophic lateral sclerosis (ALS). PLoS ONE 5:e9872. https://doi.org/10.1371/journal.pone.0009872
16. Cronin S, Berger S, Ding J, Schymick JC, Washecka N, Hernandez DG et al (2008) A genome-wide association study of sporadic ALS in a homogenous Irish population. Hum Mol Genet 17:768–774. https://doi.org/10.1093/hmg/ddm361
17. Cruts M, Gijselinck I, van der Zee J, Engelborghs S, Wils H, Pirici D et al (2006) Null mutations in progranulin cause ubiquitin-positive frontotemporal dementia linked to chromosome 17q21. Nature 442:920–924. https://doi.org/10.1038/nature05017
18. Daoud H, Valdmanis PN, Dion PA, Rouleau GA (2010) Analysis of DPP6 and FGGY as candidate genes for amyotrophic lateral sclerosis. Amyotroph Lateral Scler 11:389–391. https://doi.org/10.3109/17482960903358857
19. De Jager PL, Srivastava G, Lunnon K, Burgess J, Schalkwyk LC, Yu L et al (2014) Alzheimer's disease: early alterations in brain

DNA methylation at ANK1, BIN1, RHBDF2 and other loci. Nat Neurosci 17:1156–1163. https://doi.org/10.1038/nn.3786
20. de Majo M, Topp SD, Smith BN, Nishimura AL, Chen HJ, Gkazi AS et al (2018) ALS-associated missense and nonsense TBK1 mutations can both cause loss of kinase function. Neurobiol Aging 71:266 e210–266 e261. https://doi.org/10.1016/j.neurobiolaging.2018.06.015
21. DeJesus-Hernandez M, Mackenzie IR, Boeve BF, Boxer AL, Baker M, Rutherford NJ et al (2011) Expanded GGGGCC hexanucleotide repeat in noncoding region of C9ORF72 causes chromosome 9p-linked FTD and ALS. Neuron 72:245–256. https://doi.org/10.1016/j.neuron.2011.09.011
22. Del Bo R, Ghezzi S, Corti S, Santoro D, Prelle A, Mancuso M et al (2008) DPP6 gene variability confers increased risk of developing sporadic amyotrophic lateral sclerosis in Italian patients. J Neurol Neurosurg Psychiatry 79:1085. https://doi.org/10.1136/jnnp.2008.149146
23. DePristo MA, Banks E, Poplin R, Garimella KV, Maguire JR, Hartl C et al (2011) A framework for variation discovery and genotyping using next-generation DNA sequencing data. Nat Genet 43:491–498. https://doi.org/10.1038/ng.806
24. Diekstra FP, Van Deerlin VM, van Swieten JC, Al-Chalabi A, Ludolph AC, Weishaupt JH et al (2014) C9orf72 and UNC13A are shared risk loci for amyotrophic lateral sclerosis and frontotemporal dementia: a genome-wide meta-analysis. Ann Neurol 76:120–133. https://doi.org/10.1002/ana.24198
25. Dittwald P, Gambin T, Gonzaga-Jauregui C, Carvalho CM, Lupski JR, Stankiewicz P et al (2013) Inverted low-copy repeats and genome instability—a genome-wide analysis. Hum Mutat 34:210–220. https://doi.org/10.1002/humu.22217
26. Dobin A, Davis CA, Schlesinger F, Drenkow J, Zaleski C, Jha S et al (2013) STAR: ultrafast universal RNA-seq aligner. Bioinformatics 29:15–21. https://doi.org/10.1093/bioinformatics/bts635
27. Ferrari R, Hernandez DG, Nalls MA, Rohrer JD, Ramasamy A, Kwok JB et al (2014) Frontotemporal dementia and its subtypes: a genome-wide association study. Lancet Neurol 13:686–699. https://doi.org/10.1016/S1474-4422(14)70065-1
28. Ferrari R, Wang Y, Vandrovcova J, Guelfi S, Witeolar A, Karch CM et al (2017) Genetic architecture of sporadic frontotemporal dementia and overlap with Alzheimer's and Parkinson's diseases. J Neurol Neurosurg Psychiatry 88:152–164. https://doi.org/10.1136/jnnp-2016-314411
29. Fogh I, D'Alfonso S, Gellera C, Ratti A, Cereda C, Penco S et al (2011) No association of DPP6 with amyotrophic lateral sclerosis in an Italian population. Neurobiol Aging 32:966–967. https://doi.org/10.1016/j.neurobiolaging.2009.05.014
30. Freischmidt A, Wieland T, Richter B, Ruf W, Schaeffer V, Muller K et al (2015) Haploinsufficiency of TBK1 causes familial ALS and fronto-temporal dementia. Nat Neurosci 18:631–636. https://doi.org/10.1038/nn.4000
31. Geier EG, Bourdenx M, Storm NJ, Cochran JN, Sirkis DW, Hwang JH et al (2018) Rare variants in the neuronal ceroid lipofuscinosis gene MFSD8 are candidate risk factors for frontotemporal dementia. Acta Neuropathol. https://doi.org/10.1007/s00401-018-1925-9
32. Gorno-Tempini ML, Hillis AE, Weintraub S, Kertesz A, Mendez M, Cappa SF et al (2011) Classification of primary progressive aphasia and its variants. Neurology 76:1006–1014. https://doi.org/10.1212/WNL.0b013e31821103e6
33. Gusareva ES, Carrasquillo MM, Bellenguez C, Cuyvers E, Colon S, Graff-Radford NR et al (2014) Genome-wide association interaction analysis for Alzheimer's disease. Neurobiol Aging 35:2436–2443. https://doi.org/10.1016/j.neurobiolaging.2014.05.014
34. Hamza TH, Zabetian CP, Tenesa A, Laederach A, Montimurro J, Yearout D et al (2010) Common genetic variation in the HLA region is associated with late-onset sporadic Parkinson's disease. Nat Genet 42:781–785. https://doi.org/10.1038/ng.642
35. Hara M, Arino H, Petit-Pedrol M, Sabater L, Titulaer MJ, Martinez-Hernandez E et al (2017) DPPX antibody-associated encephalitis: main syndrome and antibody effects. Neurology 88:1340–1348. https://doi.org/10.1212/WNL.0000000000003796
36. Helgason E, Phung QT, Dueber EC (2013) Recent insights into the complexity of Tank-binding kinase 1 signaling networks: the emerging role of cellular localization in the activation and substrate specificity of TBK1. FEBS Lett 587:1230–1237. https://doi.org/10.1016/j.febslet.2013.01.059
37. Hsiung GY, Fok A, Feldman HH, Rademakers R, Mackenzie IR (2011) rs5848 polymorphism and serum progranulin level. J Neurol Sci 300:28–32. https://doi.org/10.1016/j.jns.2010.10.009
38. Hutton M, Lendon CL, Rizzu P, Baker M, Froelich S, Houlden H et al (1998) Association of missense and 5′-splice-site mutations in tau with the inherited dementia FTDP-17. Nature 393:702–705. https://doi.org/10.1038/31508
39. Kim YE, Oh KW, Noh MY, Nahm M, Park J, Lim SM et al (2017) Genetic and functional analysis of TBK1 variants in Korean patients with sporadic amyotrophic lateral sclerosis. Neurobiol Aging 50:170 e171–170 e176. https://doi.org/10.1016/j.neurobiolaging.2016.11.003
40. Komuro A, Horvath CM (2006) RNA- and virus-independent inhibition of antiviral signaling by RNA helicase LGP2. J Virol 80:12332–12342. https://doi.org/10.1128/JVI.01325-06
41. Krabbe G, Minami SS, Etchegaray JI, Taneja P, Djukic B, Davalos D et al (2017) Microglial NFkappaB-TNFalpha hyperactivation induces obsessive-compulsive behavior in mouse models of progranulin-deficient frontotemporal dementia. Proc Natl Acad Sci USA 114:5029–5034. https://doi.org/10.1073/pnas.1700477114
42. Lall D, Baloh RH (2017) Microglia and C9orf72 in neuroinflammation and ALS and frontotemporal dementia. J Clin Invest 127:3250–3258. https://doi.org/10.1172/JCI90607
43. Lambert JC, Ibrahim-Verbaas CA, Harold D, Naj AC, Sims R, Bellenguez C et al (2013) Meta-analysis of 74,046 individuals identifies 11 new susceptibility loci for Alzheimer's disease. Nat Genet 45:1452–1458. https://doi.org/10.1038/ng.2802
44. Lant SB, Robinson AC, Thompson JC, Rollinson S, Pickering-Brown S, Snowden JS et al (2014) Patterns of microglial cell activation in frontotemporal lobar degeneration. Neuropathol Appl Neurobiol 40:686–696. https://doi.org/10.1111/nan.12092
45. Lee EB, Porta S, Michael Baer G, Xu Y, Suh E, Kwong LK et al (2017) Expansion of the classification of FTLD-TDP: distinct pathology associated with rapidly progressive frontotemporal degeneration. Acta Neuropathol 134:65–78. https://doi.org/10.1007/s00401-017-1679-9
46. Lenormand C, Bausinger H, Gross F, Signorino-Gelo F, Koch S, Peressin M et al (2012) HLA-DQA2 and HLA-DQB2 genes are specifically expressed in human Langerhans cells and encode a new HLA class II molecule. J Immunol 188:3903–3911. https://doi.org/10.4049/jimmunol.1103048
47. Li H, Durbin R (2009) Fast and accurate short read alignment with Burrows–Wheeler transform. Bioinformatics 25:1754–1760. https://doi.org/10.1093/bioinformatics/btp324
48. Li X, Yang M, Yu Z, Tang S, Wang L, Cao X et al (2017) The tyrosine kinase Src promotes phosphorylation of the kinase TBK1 to facilitate type I interferon production after viral infection. Sci Signal. https://doi.org/10.1126/scisignal.aae0435
49. Liao C, Fu F, Li R, Yang WQ, Liao HY, Yan JR et al (2013) Loss-of-function variation in the DPP6 gene is associated with autosomal dominant microcephaly and mental retardation. Eur J Med Genet 56:484–489. https://doi.org/10.1016/j.ejmg.2013.06.008

50. Liao Y, Smyth GK, Shi W (2014) featureCounts: an efficient general purpose program for assigning sequence reads to genomic features. Bioinformatics 30:923–930. https://doi.org/10.1093/bioinformatics/btt656
51. Lin L, Murphy JG, Karlsson RM, Petralia RS, Gutzmann JJ, Abebe D et al (2018) DPP6 loss impacts hippocampal synaptic development and induces behavioral impairments in recognition, learning and memory. Front Cell Neurosci 12:84. https://doi.org/10.3389/fncel.2018.00084
52. Liu S, Cai X, Wu J, Cong Q, Chen X, Li T et al (2015) Phosphorylation of innate immune adaptor proteins MAVS, STING, and TRIF induces IRF3 activation. Science 347:aaa2630. https://doi.org/10.1126/science.aaa2630
53. Lui H, Zhang J, Makinson SR, Cahill MK, Kelley KW, Huang HY et al (2016) Progranulin deficiency promotes circuit-specific synaptic pruning by microglia via complement activation. Cell 165:921–935. https://doi.org/10.1016/j.cell.2016.04.001
54. Mackenzie IR, Baker M, Pickering-Brown S, Hsiung GY, Lindholm C, Dwosh E et al (2006) The neuropathology of frontotemporal lobar degeneration caused by mutations in the progranulin gene. Brain 129:3081–3090. https://doi.org/10.1093/brain/awl271
55. Mackenzie IR, Neumann M, Baborie A, Sampathu DM, Du Plessis D, Jaros E et al (2011) A harmonized classification system for FTLD-TDP pathology. Acta Neuropathol 122:111–113. https://doi.org/10.1007/s00401-011-0845-8
56. Martens LH, Zhang J, Barmada SJ, Zhou P, Kamiya S, Sun B et al (2012) Progranulin deficiency promotes neuroinflammation and neuron loss following toxin-induced injury. J Clin Invest 122:3955–3959. https://doi.org/10.1172/JCI63113
57. McKenna A, Hanna M, Banks E, Sivachenko A, Cibulskis K, Kernytsky A et al (2010) The genome analysis toolkit: a MapReduce framework for analyzing next-generation DNA sequencing data. Genome Res 20:1297–1303. https://doi.org/10.1101/gr.107524.110
58. McPeek MS, Sun L (2000) Statistical tests for detection of misspecified relationships by use of genome-screen data. Am J Hum Genet 66:1076–1094. https://doi.org/10.1086/302800
59. Miller ZA, Rankin KP, Graff-Radford NR, Takada LT, Sturm VE, Cleveland CM et al (2013) TDP-43 frontotemporal lobar degeneration and autoimmune disease. J Neurol Neurosurg Psychiatry 84:956–962. https://doi.org/10.1136/jnnp-2012-304644
60. Miller ZA, Sturm VE, Camsari GB, Karydas A, Yokoyama JS, Grinberg LT et al (2016) Increased prevalence of autoimmune disease within C9 and FTD/MND cohorts: completing the picture. Neurol Neuroimmunol Neuroinflamm 3:e301. https://doi.org/10.1212/NXI.0000000000000301
61. Nalls MA, Pankratz N, Lill CM, Do CB, Hernandez DG, Saad M et al (2014) Large-scale meta-analysis of genome-wide association data identifies six new risk loci for Parkinson's disease. Nat Genet 46:989–993. https://doi.org/10.1038/ng.3043
62. Ng PC, Henikoff S (2003) SIFT: predicting amino acid changes that affect protein function. Nucl Acids Res 31:3812–3814
63. Nicholson AM, Finch NA, Thomas CS, Wojtas A, Rutherford NJ, Mielke MM et al (2014) Progranulin protein levels are differently regulated in plasma and CSF. Neurology 82:1871–1878. https://doi.org/10.1212/WNL.0000000000000445
64. Nicolas A, Kenna KP, Renton AE, Ticozzi N, Faghri F, Chia R et al (2018) Genome-wide analyses identify KIF5A as a novel ALS gene. Neuron 97(1268–1283):e1266. https://doi.org/10.1016/j.neuron.2018.02.027
65. Ning S, Pagano JS, Barber GN (2011) IRF7: activation, regulation, modification and function. Genes Immun 12:399–414. https://doi.org/10.1038/gene.2011.21
66. O'Rourke JG, Bogdanik L, Yanez A, Lall D, Wolf AJ, Muhammad AK et al (2016) C9orf72 is required for proper macrophage and microglial function in mice. Science 351:1324–1329. https://doi.org/10.1126/science.aaf1064
67. Ohm DT, Kim G, Gefen T, Rademaker A, Weintraub S, Bigio EH et al (2018) Prominent microglial activation in cortical white matter is selectively associated with cortical atrophy in primary progressive aphasia. Neuropathol Appl Neurobiol. https://doi.org/10.1111/nan.12494
68. Olson JE, Ryu E, Johnson KJ, Koenig BA, Maschke KJ, Morrisette JA et al (2013) The Mayo Clinic Biobank: a building block for individualized medicine. Mayo Clin Proc 88:952–962. https://doi.org/10.1016/j.mayocp.2013.06.006
69. Parkinson N, Ince PG, Smith MO, Highley R, Skibinski G, Andersen PM et al (2006) ALS phenotypes with mutations in CHMP2B (charged multivesicular body protein 2B). Neurology 67:1074–1077. https://doi.org/10.1212/01.wnl.0000231510.89311.8b
70. Placek K, Baer GM, Elman L, McCluskey L, Hennessy L, Ferraro PM et al (2018) UNC13A polymorphism contributes to frontotemporal disease in sporadic amyotrophic lateral sclerosis. Neurobiol Aging 73:190–199. https://doi.org/10.1016/j.neurobiolaging.2018.09.031
71. Pottier C, Bieniek KF, Finch N, van de Vorst M, Baker M, Perkersen R et al (2015) Whole-genome sequencing reveals important role for TBK1 and OPTN mutations in frontotemporal lobar degeneration without motor neuron disease. Acta Neuropathol 130:77–92. https://doi.org/10.1007/s00401-015-1436-x
72. Project Min EALSSC (2018) Project MinE: study design and pilot analyses of a large-scale whole-genome sequencing study in amyotrophic lateral sclerosis. Eur J Hum Genet 26:1537–1546. https://doi.org/10.1038/s41431-018-0177-4
73. Purcell S, Neale B, Todd-Brown K, Thomas L, Ferreira MA, Bender D et al (2007) PLINK: a tool set for whole-genome association and population-based linkage analyses. Am J Hum Genet 81:559–575. https://doi.org/10.1086/519795
74. Rademakers R, Eriksen JL, Baker M, Robinson T, Ahmed Z, Lincoln SJ et al (2008) Common variation in the miR-659 binding-site of GRN is a major risk factor for TDP43-positive frontotemporal dementia. Hum Mol Genet 17:3631–3642. https://doi.org/10.1093/hmg/ddn257
75. Rascovsky K, Hodges JR, Knopman D, Mendez MF, Kramer JH, Neuhaus J et al (2011) Sensitivity of revised diagnostic criteria for the behavioural variant of frontotemporal dementia. Brain 134:2456–2477. https://doi.org/10.1093/brain/awr179
76. Rollinson S, Rohrer JD, van der Zee J, Sleegers K, Mead S, Engelborghs S et al (2011) No association of PGRN 3′UTR rs5848 in frontotemporal lobar degeneration. Neurobiol Aging 32:754–755. https://doi.org/10.1016/j.neurobiolaging.2009.04.009
77. Rothenfusser S, Goutagny N, DiPerna G, Gong M, Monks BG, Schoenemeyer A et al (2005) The RNA helicase Lgp2 inhibits TLR-independent sensing of viral replication by retinoic acid-inducible gene-I. J Immunol 175:5260–5268
78. Saito T, Hirai R, Loo YM, Owen D, Johnson CL, Sinha SC et al (2007) Regulation of innate antiviral defenses through a shared repressor domain in RIG-I and LGP2. Proc Natl Acad Sci USA 104:582–587. https://doi.org/10.1073/pnas.0606699104
79. Satoh T, Kato H, Kumagai Y, Yoneyama M, Sato S, Matsushita K et al (2010) LGP2 is a positive regulator of RIG-I- and MDA5-mediated antiviral responses. Proc Natl Acad Sci USA 107:1512–1517. https://doi.org/10.1073/pnas.0912986107
80. Schludi MH, Becker L, Garrett L, Gendron TF, Zhou Q, Schreiber F et al (2017) Spinal poly-GA inclusions in a C9orf72 mouse model trigger motor deficits and inflammation without neuron loss. Acta Neuropathol 134:241–254. https://doi.org/10.1007/s00401-017-1711-0
81. Simon-Sanchez J, Seelaar H, Bochdanovits Z, Deeg DJ, van Swieten JC, Heutink P (2009) Variation at GRN 3′-UTR rs5848 is

not associated with a risk of frontotemporal lobar degeneration in Dutch population. PLoS ONE 4:e7494. https://doi.org/10.1371/journal.pone.0007494
82. Sun W, Maffie JK, Lin L, Petralia RS, Rudy B, Hoffman DA (2011) DPP6 establishes the A-type K(+) current gradient critical for the regulation of dendritic excitability in CA1 hippocampal neurons. Neuron 71:1102–1115. https://doi.org/10.1016/j.neuron.2011.08.008
83. Taipa R, Brochado P, Robinson A, Reis I, Costa P, Mann DM et al (2017) Patterns of microglial cell activation in Alzheimer disease and frontotemporal lobar degeneration. Neurodegener Dis 17:145–154. https://doi.org/10.1159/000457127
84. Tobin WO, Lennon VA, Komorowski L, Probst C, Clardy SL, Aksamit AJ et al (2014) DPPX potassium channel antibody: frequency, clinical accompaniments, and outcomes in 20 patients. Neurology 83:1797–1803. https://doi.org/10.1212/WNL.0000000000000991
85. Tsai PC, Liu YC, Lin KP, Liu YT, Liao YC, Hsiao CT et al (2016) Mutational analysis of TBK1 in Taiwanese patients with amyotrophic lateral sclerosis. Neurobiol Aging 40:191 e111–191 e116. https://doi.org/10.1016/j.neurobiolaging.2015.12.022
86. Van Deerlin VM, Sleiman PM, Martinez-Lage M, Chen-Plotkin A, Wang LS, Graff-Radford NR et al (2010) Common variants at 7p21 are associated with frontotemporal lobar degeneration with TDP-43 inclusions. Nat Genet 42:234–239. https://doi.org/10.1038/ng.536
87. Van der Auwera GA, Carneiro MO, Hartl C, Poplin R, Del Angel G, Levy-Moonshine A et al (2013) From FastQ data to high confidence variant calls: the Genome Analysis Toolkit best practices pipeline. Curr Protoc Bioinformatics 43:11-10–11-33. https://doi.org/10.1002/0471250953.bi1110s43
88. van der Zee J, Gijselinck I, Dillen L, Van Langenhove T, Theuns J, Engelborghs S et al (2013) A pan-European study of the C9orf72 repeat associated with FTLD: geographic prevalence, genomic instability, and intermediate repeats. Hum Mutat 34:363–373. https://doi.org/10.1002/humu.22244
89. van der Zee J, Gijselinck I, Van Mossevelde S, Perrone F, Dillen L, Heeman B et al (2017) TBK1 mutation spectrum in an extended european patient cohort with frontotemporal dementia and amyotrophic lateral sclerosis. Hum Mutat 38:297–309. https://doi.org/10.1002/humu.23161
90. van Es MA, van Vught PW, Blauw HM, Franke L, Saris CG, Van den Bosch L et al (2008) Genetic variation in DPP6 is associated with susceptibility to amyotrophic lateral sclerosis. Nat Genet 40:29–31. https://doi.org/10.1038/ng.2007.52
91. van Es MA, Veldink JH, Saris CG, Blauw HM, van Vught PW, Birve A et al (2009) Genome-wide association study identifies 19p13.3 (UNC13A) and 9p21.2 as susceptibility loci for sporadic amyotrophic lateral sclerosis. Nat Genet 41:1083–1087. https://doi.org/10.1038/ng.442
92. van Rheenen W, Shatunov A, Dekker AM, McLaughlin RL, Diekstra FP, Pulit SL et al (2016) Genome-wide association analyses identify new risk variants and the genetic architecture of amyotrophic lateral sclerosis. Nat Genet 48:1043–1048. https://doi.org/10.1038/ng.3622
93. Venkataraman T, Valdes M, Elsby R, Kakuta S, Caceres G, Saijo S et al (2007) Loss of DExD/H box RNA helicase LGP2 manifests disparate antiviral responses. J Immunol 178:6444–6455
94. Wang J, Vasaikar S, Shi Z, Greer M, Zhang B (2017) WebGestalt 2017: a more comprehensive, powerful, flexible and interactive gene set enrichment analysis toolkit. Nucl Acids Res 45:W130–W137. https://doi.org/10.1093/nar/gkx356
95. Wang K, Li M, Hakonarson H (2010) ANNOVAR: functional annotation of genetic variants from high-throughput sequencing data. Nucl Acids Res 38:e164. https://doi.org/10.1093/nar/gkq603
96. Wang L, Wang S, Li W (2012) RSeQC: quality control of RNA-seq experiments. Bioinformatics 28:2184–2185. https://doi.org/10.1093/bioinformatics/bts356
97. Watts GD, Wymer J, Kovach MJ, Mehta SG, Mumm S, Darvish D et al (2004) Inclusion body myopathy associated with Paget disease of bone and frontotemporal dementia is caused by mutant valosin-containing protein. Nat Genet 36:377–381. https://doi.org/10.1038/ng1332
98. Wu MC, Lee S, Cai T, Li Y, Boehnke M, Lin X (2011) Rare-variant association testing for sequencing data with the sequence kernel association test. Am J Hum Genet 89:82–93. https://doi.org/10.1016/j.ajhg.2011.05.029
99. Xue B, Li H, Guo M, Wang J, Xu Y, Zou X et al (2018) TRIM21 Promotes Innate Immune Response to RNA Viral Infection through Lys27-Linked Polyubiquitination of MAVS. J Virol. https://doi.org/10.1128/jvi.00321-18
100. Yin F, Banerjee R, Thomas B, Zhou P, Qian L, Jia T et al (2010) Exaggerated inflammation, impaired host defense, and neuropathology in progranulin-deficient mice. J Exp Med 207:117–128. https://doi.org/10.1084/jem.20091568
101. Yoneyama M, Kikuchi M, Matsumoto K, Imaizumi T, Miyagishi M, Taira K et al (2005) Shared and unique functions of the DExD/H-box helicases RIG-I, MDA5, and LGP2 in antiviral innate immunity. J Immunol 175:2851–2858
102. Zanardini R, Ciani M, Benussi L, Ghidoni R (2016) Molecular pathways bridging frontotemporal lobar degeneration and psychiatric disorders. Front Aging Neurosci 8:10. https://doi.org/10.3389/fnagi.2016.00010
103. Zhang B, Kirov S, Snoddy J (2005) WebGestalt: an integrated system for exploring gene sets in various biological contexts. Nucl Acids Res 33:W741–W748. https://doi.org/10.1093/nar/gki475

Affiliations

Cyril Pottier[1] · Yingxue Ren[2] · Ralph B. Perkerson III[1] · Matt Baker[1] · Gregory D. Jenkins[3] · Marka van Blitterswijk[1] · Mariely DeJesus-Hernandez[1] · Jeroen G. J. van Rooij[4] · Melissa E. Murray[1] · Elizabeth Christopher[1] · Shannon K. McDonnell[3] · Zachary Fogarty[3] · Anthony Batzler[3] · Shulan Tian[3] · Cristina T. Vicente[1] · Billie Matchett[1] · Anna M. Karydas[5] · Ging-Yuek Robin Hsiung[6] · Harro Seelaar[4] · Merel O. Mol[4] · Elizabeth C. Finger[7] · Caroline Graff[8,9] · Linn Öijerstedt[8,9] · Manuela Neumann[10,11] · Peter Heutink[10,12] · Matthis Synofzik[10,12] · Carlo Wilke[10,12] · Johannes Prudlo[10,13] · Patrizia Rizzu[10] · Javier Simon-Sanchez[10,12] · Dieter Edbauer[14,15] · Sigrun Roeber[16] · Janine Diehl-Schmid[17] · Bret M. Evers[18] · Andrew King[19,20] · M. Marsel Mesulam[21] · Sandra Weintraub[21,22] · Changiz Geula[21] · Kevin F. Bieniek[1,23] · Leonard Petrucelli[1] · Geoffrey L. Ahern[24] · Eric M. Reiman[25] · Bryan K. Woodruff[26] · Richard J. Caselli[26] · Edward D. Huey[27] · Martin R. Farlow[28] · Jordan Grafman[29] · Simon Mead[30] · Lea T. Grinberg[5,31] · Salvatore Spina[5] · Murray Grossman[32] · David J. Irwin[32] ·

Edward B. Lee[33] · EunRan Suh[33] · Julie Snowden[34] · David Mann[35] · Nilufer Ertekin-Taner[1,36] · Ryan J. Uitti[36] · Zbigniew K. Wszolek[36] · Keith A. Josephs[37] · Joseph E. Parisi[37] · David S. Knopman[37] · Ronald C. Petersen[37] · John R. Hodges[38] · Olivier Piguet[39] · Ethan G. Geier[5] · Jennifer S. Yokoyama[5] · Robert A. Rissman[40,41] · Ekaterina Rogaeva[42] · Julia Keith[43,44] · Lorne Zinman[43] · Maria Carmela Tartaglia[42,45] · Nigel J. Cairns[46] · Carlos Cruchaga[47] · Bernardino Ghetti[48] · Julia Kofler[49] · Oscar L. Lopez[50,24] · Thomas G. Beach[51] · Thomas Arzberger[52,14,16] · Jochen Herms[14,16] · Lawrence S. Honig[53] · Jean Paul Vonsattel[54] · Glenda M. Halliday[38,55] · John B. Kwok[38,55] · Charles L. White III[18] · Marla Gearing[56] · Jonathan Glass[56] · Sara Rollinson[57] · Stuart Pickering-Brown[57] · Jonathan D. Rohrer[58] · John Q. Trojanowski[33] · Vivianna Van Deerlin[33] · Eileen H. Bigio[21] · Claire Troakes[19] · Safa Al-Sarraj[19,20] · Yan Asmann[2] · Bruce L. Miller[5] · Neill R. Graff-Radford[36] · Bradley F. Boeve[37] · William W. Seeley[5,31] · Ian R. A. Mackenzie[59] · John C. van Swieten[4] · Dennis W. Dickson[1] · Joanna M. Biernacka[3] · Rosa Rademakers[1]

✉ Rosa Rademakers
Rademakers.rosa@mayo.edu

[1] Department of Neuroscience, Mayo Clinic, 4500 San Pablo Road, Jacksonville, FL 32224, USA

[2] Department of Health Sciences Research, Mayo Clinic, Jacksonville, FL, USA

[3] Department of Health Sciences Research, Mayo Clinic, Rochester, MN, USA

[4] Department of Neurology, Erasmus Medical Center, Wytemaweg 80, 3015 CN Rotterdam, The Netherlands

[5] Department of Neurology, Memory and Aging Center, University of California, San Francisco, CA, USA

[6] Division of Neurology, Department of Medicine, University of British Columbia, Vancouver, BC V6T 2B5, Canada

[7] Department of Clinical Neurological Sciences, Schulich School of Medicine and Dentistry, University of Western Ontario, London, ON N6A 2E2, Canada

[8] Division of Neurogeriatrics, Department NVS, Karolinska Institutet, Visionsgatan 4, J10:20, 171 64 Solna, Sweden

[9] Theme Aging, Unit for Hereditary Dementias, Karolinska University Hospital, Solna, Sweden

[10] German Center for Neurodegenerative Diseases (DZNE), 18147 Rostock, Germany

[11] Department of Neuropathology, University of Tübingen, 72076 Tübingen, Germany

[12] Hertie Institute for Clinical Brain Research, University of Tübingen, 72076 Tübingen, Germany

[13] Department of Neurology, Rostock University Medical Center, 18147 Rostock, Germany

[14] German Center for Neurodegenerative Diseases (DZNE), Feodor-Lynen-Str 17, 81377 Munich, Germany

[15] Munich Cluster of Systems Neurology (SyNergy), Feodor-Lynen-Str 17, 81377 Munich, Germany

[16] Center for Neuropathology and Prion Research, Ludwig-Maximilians-University of Munich, Feodor-Lynen-Straße 23, 81377 Munich, Germany

[17] Department of Psychiatry and Psychotherapy, Technische Universität München, Munich, Germany

[18] Division of Neuropathology, University of Texas Southwestern Medical Center, 5323 Harry Hines Blvd, Dallas, TX 75390-9073, USA

[19] London Neurodegenerative Diseases Brain Bank, Department of Basic and Clinical Neuroscience, Institute of Psychiatry, Psychology and Neuroscience, King's College London, London SE5 8AF, UK

[20] Department of Clinical Neuropathology, King's College Hospital NHS Foundation Trust, London SE5 9RS, UK

[21] Mesulam Center for Cognitive Neurology and Alzheimer's Disease, Northwestern University, Chicago, IL 60611, USA

[22] Department of Psychiatry and Behavioral Sciences and Department of Neurology, Northwestern University Feinberg School of Medicine, Chicago, IL 60611, USA

[23] Glenn Biggs Institute for Alzheimer's and Neurodegenerative Diseases, University of Texas Health Science Center San Antonio, San Antonio, TX 78229, USA

[24] Department of Neurology, University of Arizona Health Sciences Center, 1501 North Campbell Avenue, Tucson, AZ 85724-5023, USA

[25] Banner Alzheimer's Institute, Phoenix, AZ 85006, USA

[26] Department of Neurology, Mayo Clinic Arizona, Scottsdale, AZ 85259, USA

[27] Departments of Psychiatry and Neurology, Taub Institute for Research on Alzheimer's Disease and the Aging Brain, Columbia University, 630 West 168th St P&S Box 16, New York, NY 10032, USA

[28] Indiana University School of Medicine, 355 West 16th Street, GH 4700 Neurology, Indianapolis, IN 46202, USA

[29] Department of Physical Medicine and Rehabilitation, Neurology, Cognitive Neurology and Alzheimer's Center, Department of Psychiatry, Feinberg School of Medicine, Northwestern University, 355 E Erie Street, Chicago, IL 60611-5146, USA

[30] MRC Prion Unit at University College London, Institute of Prion Diseases, London, UK

[31] Department of Pathology, Memory and Aging Center, University of California, San Francisco, CA, USA

[32] Penn Frontotemporal Degeneration Center, Department of Neurology, Perelman School of Medicine at the University of Pennsylvania, Philadelphia, PA 19104, USA

[33] Center for Neurodegenerative Disease Research, Department of Pathology and Laboratory Medicine, Perelman School of Medicine at the University of Pennsylvania, Philadelphia, PA 19104, USA

[34] Cerebral Function Unit, Greater Manchester Neurosciences Centre, Salford Royal Hospital, Salford, UK

[35] Division of Neuroscience and Experimental Psychology, School of Biological Sciences, Faculty of Biology, Medicine and Health, University of Manchester, Salford Royal Hospital, Salford, UK

[36] Department of Neurology, Mayo Clinic, Jacksonville, FL, USA

[37] Department of Neurology, Mayo Clinic, Rochester, MN, USA

[38] Central Clinical School and Brain and Mind Centre, The University of Sydney, Sydney 2050, Australia

[39] School of Psychology and Brain and Mind Centre, The University of Sydney, Sydney 2050, Australia

[40] Department of Neurosciences, University of California, San Diego, La Jolla, CA 92093, USA

[41] Veterans Affairs San Diego Healthcare System, San Diego, CA 92161, USA

[42] Krembil Discovery Tower, Tanz Centre for Research in Neurodegenerative Disease, University of Toronto, 60 Leonard Av, 4th Floor - 4KD481, Toronto, ON M5T 0S8, Canada

[43] Sunnybrook Health Sciences Centre, Toronto, ON M4N 3M5, Canada

[44] Department of Laboratory Medicine and Pathobiology, University of Toronto, Toronto, ON M5S 1A1, Canada

[45] Krembil Neuroscience Center, Movement Disorder's Clinic, Toronto Western Hospital, 399 Bathurst Street, Toronto, ON M5T 2S8, Canada

[46] Department of Neurology, Knight Alzheimer Disease Research Center, Washington University School of Medicine, Saint Louis, MO 63108, USA

[47] Department of Psychiatry, Knight Alzheimer Disease Research Center, Washington University School of Medicine, Saint Louis, MO 63108, USA

[48] Department of Pathology and Laboratory Medicine, Indiana University School of Medicine, 635 Barnhill Drive, MS A138, Indianapolis, IN 46202, USA

[49] Department of Pathology, University of Pittsburgh, Pittsburgh, PA 15213, USA

[50] Department of Neurology, University of Pittsburgh, Pittsburgh, PA 15213, USA

[51] Civin Laboratory for Neuropathology, Banner Sun Health Research Institute, Sun City, AZ 85351, USA

[52] Department of Psychiatry and Psychotherapy, University Hospital, Ludwig-Maximilians-University of Munich, Nussbaumstraße 7, 80336 Munich, Germany

[53] Department of Neurology, Taub Institute, and GH Sergievsky Center, Columbia University Irving Medical Center, 630 West 168th St (P&S Unit 16), New York, NY 10032, USA

[54] Department of Pathology and Taub Institute, Columbia University Irving Medical Center, 630 West 168th St, New York, NY 10032, USA

[55] UNSW Medicine and NeuRA, Randwick 2031, Australia

[56] Department of Pathology and Laboratory Medicine and Department of Neurology, Emory University, Atlanta, GA 30322, USA

[57] Division of Neuroscience and Experimental Psychology, School of Biological Sciences, Faculty of Biology, Medicine and Health, University of Manchester, Manchester, UK

[58] Dementia Research Centre, Department of Neurodegenerative Disease, UCL Queen Square Institute of Neurology, London, UK

[59] Department of Pathology and Laboratory Medicine, University of British Columbia, Vancouver, BC V5Z 1M9, Canada